Universidade de Lisboa

Faculdade de Farmácia

CHARACTERIZATION OF STARCH AMORPHOUS SOLID DISPERSIONS MANUFACTURED VIA HOT-MELT EXTRUSION BY CALORIMETRY AND DIFFRACTOMETRY

Rita da Luz Franco de Paiva Duarte

Mestrado Integrado em Ciências Farmacêuticas

2020

Universidade de Lisboa

Faculdade de Farmácia

CHARACTERIZATION OF STARCH AMORPHOUS SOLID DISPERSIONS MANUFACTURED VIA HOT-MELT EXTRUSION BY CALORIMETRY AND DIFFRACTOMETRY

Rita da Luz Franco de Paiva Duarte

Monografia de Mestrado Integrado em Ciências Farmacêuticas apresentada à Universidade de Lisboa através da Faculdade de Farmácia

Orientador: Professor (Full) Karl Gerhard Wagner of University of Bonn, Germany

Co-orientado: Professor Associado, João Fernandes de Abreu Pinto

2020

Resumo

Uma tarefa desafiadora para a indústria farmacêutica tem sido a melhoria da solubilidade de fármacos pouco solúveis em água. A produção de dispersões sólidas amorfas constitui uma das estratégias mais promissoras para aumentar a solubilidade, velocidade de libertação e biodisponibilidade destes fármacos.

Este estudo propõe a produção de dispersões sólidas amorfas com fármacos de classe II do Sistema de Classificação Biofarmacêutica, através da extrusão a quente, tecnologia que permite o aumento da solubilidade em água, usando um polímero natural e biodegradável, o amido.

Os fármacos em estudo, Ibuprofeno e Carbamazepina, classificados como fármacos de classe II (baixa solubilidade e elevada permeabilidade), foram formulados com amido de milho e amido de milho glutinoso. O amido é constituído por dois biopolímeros, amilose, uma macromolécula linear, e amilopectina, uma macromolécula altamente ramificada. O Ibuprofeno e a água foram usados pelos seus efeitos plastificantes.

Primeiro, a mistura das formulações foi feita num misturador de tambor. A calorimetria diferencial de varrimento foi usada para determinar a temperatura de transição vítrea dos amidos. Durante a extrusão, a água foi adicionada ao extrusor de duplo parafuso co-rotativo através de uma bomba. Depois, as amostras foram secadas em estufa a 40°C durante ±12h e a moagem foi feita em almofariz e num moinho de bolas. Apresenta-se uma visão geral dos métodos de caracterização, a Calorimetria diferencial de varrimento e a Difração de Raios-X, para uma melhor compreensão das dispersões sólidas à base de amido.

Os dados apresentados sugerem que a maiores rotações e com mais água, os produtos extrudados tornaram-se mais amorfos. Visualmente, a maioria das amostras exibia uma cor branca opaca homogénea, característica de um material cristalino. Os resultados da difratometria das dispersões sólidas de Ibuprofeno e Carbamazepina indicam que permaneceram na sua forma cristalina. Os termogramas, que exibem um pico endotérmico, indicam de que o Ibuprofeno permaneceu cristalino.

Este trabalho permitiu uma melhor compreensão do processo de extrusão a quente, dos métodos de caracterização do estado sólido e do comportamento de amido extrudado com fármacos. Comparando os dois tipos de amidos, o amido de milho revelou-se uma melhor escolha para a produção de dispersões sólidas amorfas.

Palavras-chave: Amido, Biodisponibilidade, Dispersão sólida, Extrusão a quente, Solubilidade.

Abstract

A challenging task for the pharmaceutical industry remains the effort to improve the solubility of poorly water-soluble drugs. The production of amorphous solid dispersions is one of the most promising strategies to enhance the drug release rate and bioavailability of these active pharmaceutical ingredients.

The current study explored the production of amorphous solid dispersions with Biopharmaceutical Classification System class II drugs via hot-melt extrusion, an aqueous-solubility enhancement technology, using a natural and eco-friendly polymer such as starch.

As model drugs, Ibuprofen and Carbamazepine, categorized as class II drugs (low solubility, high permeability) were formulated with two different starch types, Maize Corn Starch and Waxy Corn Starch. Starch is made of two biopolymers, amylose, a linear macromolecule, and the highly branched amylopectin. Ibuprofen and the addiction of water had plasticizing effects.

Prior to extrusion, the physical mixtures were mixed in a tumble blender and Differential Scanning Calorimetry was used to assess the glass transition temperature of both starches. During the extrusion, water was fed into the co-rotating twin-screw with a pump. Then, the samples were dried in an oven at 40°C for ±12h, and grinding was performed through hand grinding and a ball mill. An overview of the solid-state characterization methods, Differential Scanning Calorimetry and X-Ray Powder Diffraction, is put together for a better comprehension of the extrudates' solid-state.

The data presented suggest that at a higher rotation and with more water, the extrudates became more amorphous. The visual evaluation shows most samples exhibited a white opaque homogeneous colour, characteristic of a crystalline material. The diffractograms showed that Ibuprofen and Carbamazepine were embedded in the starch matrix in their crystalline form. The thermograms of Ibuprofen solid dispersions exhibited a single sharp endothermic peak, indicating that the drug remained crystalline.

This work allowed for a better insight into the hot-melt extrusion process, the characterization methods and further understanding of the thermodynamic behaviour of hot-melt extruded starches with incorporated drugs. Comparing both starches, Maize Corn Starch revealed itself a better choice to produce amorphous solid dispersions.

Key-words: Bioavailability, formulation development, hot-melt extruded starch, solid dispersion, poorly water-soluble drugs.

Acknowledgments

Ao meu orientador, Prof. Dr. Karl Wagner, ao Prof. Dr. Hubert Rein e
aos alunos de doutoramento do Departamento de Tecnologia Farmacêutica da
Universidade de Bonn na Alemanha,

Por me darem a orientação que precisava.

Ao meu Co-orientador, Professor Doutor João F. Pinto,

Por me guiar na redação deste trabalho.

À minha mãe e ao meu pai

Pela paciência, proteção constantes e por acreditarem sempre em mim.

Aos meus amigos e colegas de curso,

Pela cumplicidade e por partilharem comigo estes cinco anos.

Ao Gaspar,

Por todo o apoio e motivação.

À minha irmã,

Pela ajuda e amizade.

Contents

List of Figures

List of Tables

Abbreviations

API – Active Pharmaceutical Ingredient

ASD – Amorphous Solid Dispersion(s)

BA – Bioavailability

BCS – Biopharmaceutics Classification System

C_{max} – Maximum plasma drug concentration

DP – Degree of Polymerization

DSC – Differential Scanning Calorimetry

EMA – European Medicines Agency

FTIR – Fourier-Transform Infrared Spectroscopy

HME – Hot-Melt Extrusion

HPLC – High performance liquid chromatography

MS – Mass Spectrometry

PM – Physical mixture

T_{deg} – Degradation Temperature

T_e – Endset Temperature

T_g – Glass Transition Temperature

T_m – Melting Temperature

t_{max} – Time required to achieve the maximal concentration

T_o – Onset Temperature

T_p – Peak Temperature

SD – Solid Dispersion

ssHME – single-screw Hot-Melt Extrusion

tsHME – twin-screw Hot-Melt Extrusion

WHO – World Health Organization

XRPD – X-Ray Powder Diffraction

1. Introduction

1.1 Amorphous Solid Dispersions

In its solid-state, active pharmaceutical ingredients (APIs) can exist in crystalline or amorphous structures. The structure of an amorphous solid possesses usually crystal-like short-range molecular arrangement but lacking the long-range order (translational-orientational symmetry) that characterizes a crystal. The crystalline form has high purity and stability. However, to dissolve the crystalline form, its lattice energy barrier must be overcome, which leads to slower drug dissolution and is a major drawback in drug development. The crystalline lattice of a poorly water-soluble drug must suffer disruption and rearrangement to convert the compound to a non-crystalline drug. This is an endothermic step that requires high energy to disrupt the crystalline arrangement.

The non-crystalline state of the drug is physically unstable and shows a tendency to revert to its crystalline state. As a consequence of secondary nucleation or growth of crystals, de-supersaturation results in a reduced amount of dissolved drug available for absorption. As both stability and dissolution performance may be undermined by the presence of seed crystals, it is considered critical to design the amorphous solid dispersions' (ASD) manufacturing process to generate a fully amorphous system. Amorphous forms have a higher molecular mobility and energy state, which gives them a higher dissolution rate and solubility. They also reveal a higher Gibbs free energy, which means they are less stable chemically and physically. For that reason, they show a greater tendency to recrystallize during the storage process. (1–4)

According to the Biopharmaceutics Classification System (BCS), a high percentage of drug development candidates, as well as marketed APIs, exhibit poor oral bioavailability and are classified as class II/IV substances because of their high/low permeability and low solubility. The poor aqueous solubility and dissolution rate of BCS Class II/IV molecules are rate-limiting steps for absorption, which generally leads to low bioavailability (BA) and their failure as drug candidates To overcome solubility issues and increase the likeliness of low-solubility drugs as viable options for further drug development, diverse approaches have been employed, such as stabilizing an API in an amorphous system by embedding it into a solid polymer matrix. (1,5,6)

The formulation of ASD, the dispersion of an API in an inert carrier or matrix and the conversion of the crystalline drug into its amorphous form is a promising strategy to the low solubility problem. To obtain a stable ASD, the drug and the polymer must be in a liquid state, through melting or dissolution then properly mixed and finally solidified. The result is a kinetic entrapment of the drug in its amorphous state. A fraction of the drug might molecularly disperse in the matrix, thereby forming a solid dispersion. When the solid dispersion is exposed to

aqueous media, the carrier dissolves and the drug is released. In contrast to its crystalline form, the resulting enhanced surface area produces a higher dissolution rate and bioavailability of poorly water-soluble drugs. (1,5,7,8)

The API with poor dissolution, incomplete absorption, and reduced bioavailability can be mixed with a polymer at a molecular level to form an ASD. The latter has an enhanced dissolution, better absorption and bioavailability and is suitable for a broad range of final dosage forms, which makes ASD a highly desirable product for the pharmaceutical industry. (9) First, the formation of ASD is one of the reliable, robust, and reproducible techniques for improving solubility and bioavailability. Secondly, ASD not only offer the inherent free energy benefit but also provide maximum increase in surface area and saturation solubility, which allows the solvent to be cavitated at a higher rate and extent (solvent cavitation involves the creation of space in the solvent to host the drug molecules. This is also an endothermic step. The rate and extent of solvent cavitation is higher for a drug embedded in an ASD compared to a crystalline or neat amorphous drug. This is because the hydrophilic polymers aid in the reduction of surface tension between the drug and solvent, thereby making larger cavities in the solvent more quickly) resulting in higher API solubility and bioavailability. Besides, the polymer used can inhibit the drug precipitation in the aqueous media. (3,10,11)

The manufacturing of ASD turns poorly soluble crystalline APIs into better formulations, because the physical form of the API is stabilized by the polymers used, and allows for the development of more successful treatments. (5) Scientists have already tried to address solubility issues by various pharmaceutical interventions. There are several methods for manufacturing ASDs based on heating (e.g., hot melt extrusion) or based on solvents (e.g., spray-drying, freeze drying, thin-film freezing, co-precipitation or electro-spinning). Among the many methods available to improve solubility and dissolution rate, HME has gained vast attention and has been successfully applied to prepare solid molecular dispersions of APIs into different polymer matrices. (3,12)

1.2   Hot-Melt Extrusion

Processes that introduce mechanical stress can render crystalline materials fully or partially amorphous, thus process conditions can influence the amount of amorphous materials in the end product. (2)

Extrusion is the process of pumping raw materials at elevated controlled temperature and pressure through a barrel for material transport, mixing and conversion of blends from a powder or a granular mix into a product of uniform density. During this process, polymers are melted and formed under controlled temperature, pressure, feeding rate, and screw speed into products of different shapes and sizes such as plastic bags, sheets, and pipes by forcing

polymeric components and active substances including any additives or plasticizers through an orifice or die. An end-plate die is connected to the end of the barrel and shapes the extruded materials exiting the barrel. (12) More recently, 3D printing technologies and injection molding have been developed as natural evolutions of these classic HME technologies. (13)

An extruder is typically composed of a feeding hopper, a stationary cylindrical barrel, single or twin-screws, the die and screw–driving unit (Fig. 1). The auxiliary equipment consists of a heating/cooling device for the barrels, a conveyor belt to cool down the product and a solvent delivery pump. The monitoring devices on the equipment include temperature and pressure gauges, a screw-speed controller, an extrusion torque monitor. (14)

The conveying system transports the material through the barrel via the action of Archimedes' infinite screws and sometimes imparts a degree of distributive mixing and dispersion; and a dye system that forms the materials into the required shape. The die is a metal conduit at the output area of the extruder, with a constant cross-sectional area, a narrow opening with a constant diameter, where the extrudate strand flows through. (8,15)
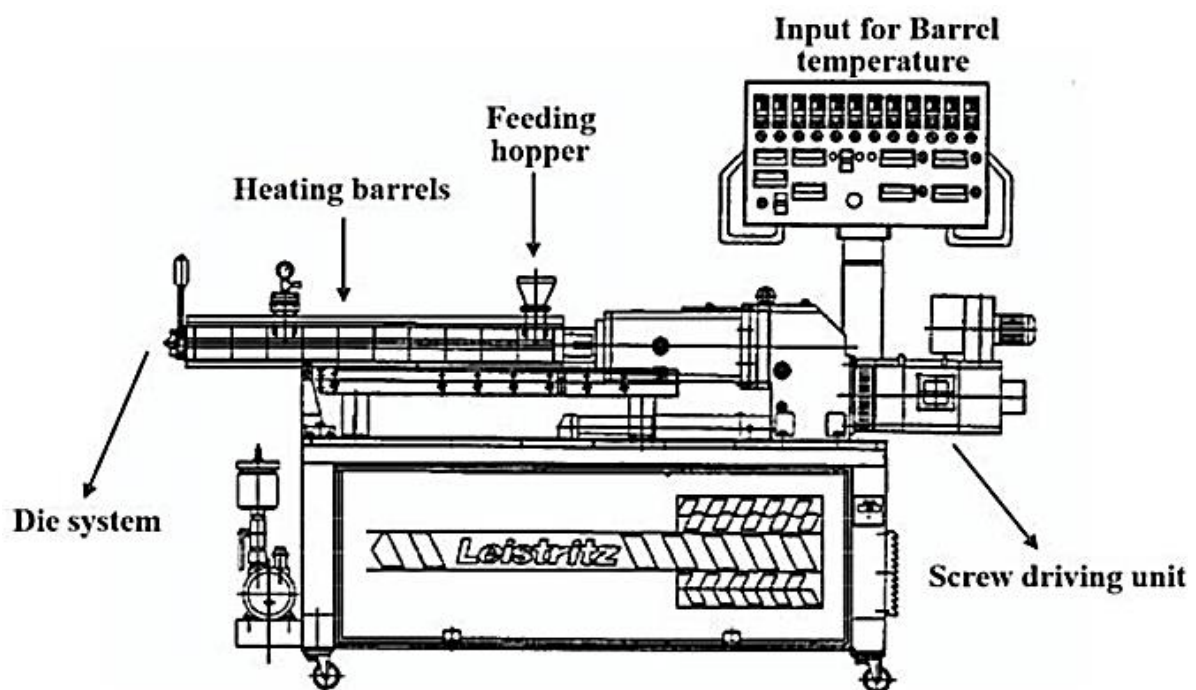
Figure 1. Co-rotating Twin-screw extruder. From (14).

The screws have several conveyor zones alternated with kneading elements. The kneading disks are a discontinuous unit that allows mixing and provides high shearing stress. The screws have various mixing elements which impart two types of mixing, distributive mixing and dispersive mixing. The distributive mixing ideally maximizes division, providing a uniform concentration of all components while minimizing energy. The dispersive mixing breaks aggregates into fine particles using energy. (14) In a twin-screw extruder, 90˚ kneading blocks

have no conveying effect, so the molten material stagnates and becomes very well homogenized. Furthermore, the use of 45° reverse conveying and 45° forward-conveying kneading blocks will increase the level of mixing, while the conveying element only transports the molten material through the barrel. The rotation of the twin-screws (Fig. 2) inside the extruder barrel may be either co-rotating (same direction) or counter-rotating (opposite direction). (15)
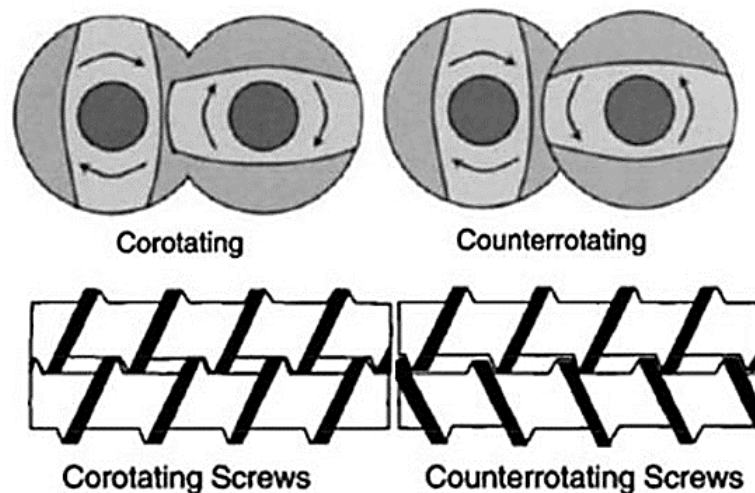
Figure 2. Screw rotation direction, co-rotating and counter-rotating screws. From (14).

The extrusion process begins with premixed drug and polymer, the polymer softens into a continuous molten phase with suspended drug particles. The heat that is generated from friction force is required to melt the material. This force is a shear force occurring between the rotating screws and the wall of the barrel that is mounted with electric or liquid heaters. (14) A dissolution boundary layer forms at the crystal-polymer interface, which drug molecules diffuse through into the melt. Similarly, the heat transfer boundary layer will also exist. These boundary layers are reduced by mixing forces. Thus, the drug crystals decrease in size until all drug molecules are molecularly dispersed in the molten polymer. Contributions from dispersive mixing may also cause breakage if the drug particle encounters the impact zone of the mixing elements or if the shear stress exceeds the critical breakage stress of the drug particles. The use of higher screw speed and shear will decrease the boundary layer thickness, facilitating dissolution and attainment of a homogenous molecular dispersion. (4)

1.2.1. Applications of HME in Pharmaceutical Research

Hot-melt extrusion (HME) has found its place in the manufacturing of ASD systems. First developed and used in the plastics industry, HME has been applied in the pharmaceutical industry as a simple, reproducible, and fast method for producing many solid dosage forms of drugs. It was first introduced in the pharmaceutical industry as an alternative to solvent-depended processes. Compared with other traditional solvent-based methods for the

manufacture of ASD, that need subsequent drying steps, is the only solvent-free technology leaving a small footprint. Since it allows a continuous process, fewer steps are involved, reducing production costs and making scaling-up easier. (5,13,15–17)

In HME, the physical mixture of drug, polymer, and, if necessary, other excipients is filled in the hopper and is conveyed, mixed, and melted as it passes through the equipment (for example, ram extrusion, single-screw or twin-screw extruder) at an elevated temperature, where the drug dissolves in the amorphous polymer with the aid of temperature and shear. When the semisolid melt is passed through the die located at the end of the extruder barrel, it shapes the molten mass in the required form such as pellets, strands or filaments that are solidified upon cooling and milled into granules for further downstream processes. (8,9,13,15)

Possible excipients are bulking agents, matrix carriers, antioxidants, thermal lubricants, plasticizers and additives. The most common additives are plasticizers, which facilitate the extrusion process by reducing the glass transition temperature of the polymers and increase the dissolution rate of HME products through plasticization and solubilisation effects. (3,15,16)

Some of the most widely developed applications are for:

1. Taste masking

2. Improved dissolution of poorly soluble drugs

3. Modified release formulations (13)

HME has been successfully applied to enhance the solubility of poorly soluble APIs and to optimize product efficiency by producing a stable ASD with increased-energy form. The resulting product, called the extrudate, is then collected for downstream processing and converted into a final dosage form to achieve the final drug delivery profile desired. (10)

1.2.2. Advantages and Disadvantages of HME

A great advantage of this process is that it generates a highly homogeneous dispersed product with desired properties, the dispersed API in the ASD exhibits a higher dissolution rate than the parent crystalline drug because no crystalline lattice bonds or interactions need to be broken. (9,16)

The advantages of HME include shorter residence time of the drug carrier mix, continuous operation possibility, good control of operating parameters, and possibility to scale up. Additionally, this production method is useful from an ecological standpoint. The absence of organic solvents and minimum product wastage make it a green technology. (8)

The release of the API and the quality of the final product can be fine-tuned by modifying the excipients. For example, some polymers have a different dissolution pH, which can allow the targeting of a specific part of the gastrointestinal tract. Some polymers can also control the release of the API in order to observe an immediate, delayed or sustained release. Another

very important aspect to bear in mind is the affinity between the API and the polymer matrix, especially when aiming for the enhancement of the bioavailability of poorly soluble drugs. (15)

Due to the intense mixing during HME, uniform dispersion of the drug improves the drug homogeneity in the final dosage form. (13) Depending on the miscibility of the drug with the polymer, different types of solid dispersions may be formed. It has been reported that extruding miscible components results in amorphous solid solution formation, whereas extrusion of an immiscible component leads to an amorphous dispersed drug in a crystalline excipient. The process has been useful as a single step approach in the preparation of solid dispersions. (8,17)

Another great advantage of the HME process is that the external shape of the products can be varied by exchanging the geometry of the nozzle, which opens a broad field of applications. Die plates can also be easily exchanged to alter the extrudate diameter. Potential applications already described in the literature are the production of oral capsules, oral matrices, implantable matrices, or intra-vaginal inserts. (14,18)

Nonetheless, HME has some disadvantages, namely, the high process temperatures (which may lead to thermal degradation of ingredients), the need for downstream processing, and the high energy input. Moreover, it presents unique challenges due to the metastable nature of the drug product produced. Its use is limited because of its difficulty in processing thermally labile drugs. (5,15)

Also, the mixture that melts under extrusion must have good flow properties through the extrusion chamber. During HME, the high energy input coming from the applied shear forces can degrade the API or the excipients. The degradation rate is directly proportional to the temperature. Besides, the mechanical energy produced by the kneading elements of the extruder can impose a sizable degree of degradation on shear-sensitive substances depending on the screw speed. Therefore, all the components must be stable under shear forces. (1,13)

These variable levels of shear applied to the materials within the extruder can have different effects, ranging from the simple mixing of the API with the polymer to the dispersion of the drug into the polymer at the molecular level, with the possibility of drug-polymer interactions. In this case, amorphous or crystalline solid dispersions are produced, which is one of the most important benefits of using tsHME (twin-screw hot-melt extrusion). This method can therefore be used to enhance the bioavailability of poorly soluble drugs. (15)

As with other breakthrough innovations, it is still an emerging technology and its potential has not yet been fully explored. (5) HME-related patents issued for pharmaceutical systems have steadily increased since the early 1980s. So far, the USA and Germany hold approximately more than half (56%) of all issued patents for HME in the market. (12)

1.2.3. Extrusion process parameters

One of the most important variables during HME is the process temperature, which depends on several factors, such as the melting of the mixture and the flowability of the mass being extruded. Frequently, the process design requires a higher operating temperature in order to obtain the rheological properties needed to allow the extrusion. Even if this temperature is decreased by the addition of specific additives such as plasticizers, nevertheless relative high temperatures are often necessary, and they affect the thermal stability of the mixture. Thus, during the process design, a balance between process feasibility and possible mixture degradation must be considered. (13) An equilibrium must be found between, on the one hand, a low temperature where the melt shows high viscosity, and thus a high torque, and on the other hand, an elevated temperature where the torque is reduced due to the low viscosity of the melt but where both the polymer and the API could be degraded. Some research papers demonstrated that working at higher temperatures facilitated the extrusion process by reducing the torque and the pressure at the die. The polymer must be processed above its T_g but also below its degradation temperature (T_{deg}). Besides, the extrusion temperature should be at least 15°C higher than the T_g of the mixture. The ideal extrusion temperature needs to be determined for each polymer/API mixture. The same goes for the API, albeit it can be processed below or above its T_m depending on whether a miscibility regime or a solubilisation regime, respectively, is being used. (1,15,16)

However, the high thermal and mechanical energy applied to the mixture during extrusion can degrade drugs or excipients. Given the high temperatures applied and the absence of solvents in the HME process, the most frequent unwanted reactions are oxidation and peroxidation, which affect drug chemical stability. The World Health Organization (WHO) recommends that the chemical and thermal stability of the product be evaluated to identify any degradation species in medicinal finished products. Chromatographic techniques, such as high-performance liquid chromatography (HPLC), are mainly devoted to evaluating the chemical stability of mixture components subjected to high temperature and shear stresses. HPLC is the most appropriate method for discovering any drug degradation and it can be equipped with different detectors, the most important of which is mass spectrometry (MS), because it may enable identification of degradation products. (13)

The type of feeder is also very important, since a gravimetric feeder, that relies on weighing the material to achieve a required discharge rate, is more precise than a volumetric one. Volumetric feeding is suitable for many solid feeding applications where accuracy is not a critical factor in the process. Generally, gravimetric feeding systems use a volumetric feeder connected to a weighing system to control the amount of powder exiting from a storage hopper at a constant weight per unit of time. (15)

Screw configuration is a very important parameter in the amorphization of the API using tsHME. The residence time of the mixture in the barrel will also be influenced by the type of element used during the process. For example, more kneading elements will increase the residence time. In their study, Nakamichi et al. (19) showed that kneading paddle elements affect the preparation of SD, play a role in the mechanical shear and a longer stay in the machine and concluded that at least one mixing zone was needed in order to obtain smooth and homogeneous extrudates while processing nifedipine (NP) and hydroxypropylmethylcellulosephthalate (HPMCP) with the kneading paddle positioned at the level of the second third of the barrel. The samples were recovered from the screw directly and analysed by DSC and X-ray diffraction (XRD).

Regarding the processing of thermally labile drug compounds, Gosh et al. (15) concluded that the position of the kneading block during tsHME was important. Indeed, the authors found that when the kneading block was positioned close to the feeding section, the API melted earlier. This meant that the API stayed longer in the barrel, thereby inducing the degradation of the compound. However, when the kneading block was positioned close to the end of the barrel, a delay in API melting was observed, and this improved the stability of the API.

Screw type, configuration and design do affect the various factors involved in the extrusion process. Generally, a high mixing capacity and a high shear screw configuration have been shown to give the best results. As far as amorphization and cocrystallization are concerned, tsHME is preferred to ssHME, since this method demonstrates a better mixing capacity. The geometry of the tsHME favours a very high degree of mixing as the surfaces of the screws move towards each other and the residence time of the mass is increased. The twin-extruder offers greater versatility, as it can process a wider range of pharmaceutical formulations. Moreover, one kneading zone positioned at the two-third or the end of the barrel is generally sufficient to facilitate a good mixing at the molecular level and to obtain high-quality cocrystals and ASD. (13,15)

In another study, Reitz et al. (15) used tsHME to extrude mannitol and GRIS and concluded that screw speed affected the load of the barrel, the mixing in the extrusion barrel, and the shear rate of the extrusion process. Moreover, the authors also found that screw speed, like temperature, influenced the flow rate, which had an impact on the residence time.

Reitz et al. (15) showed that increasing the screw speed within tsHME increased the convection and thus the transport rate related to mixing and that this decreased the residence time of the material in the extrusion barrel. Crowley et al. went even further and demonstrated the necessity of finding a suitable screw speed. A low screw speed induced polymer degradation due to the longer residence time. When increasing the screw speed, the melt viscosity of the polymer was found to decrease until the polymer melt fracture was reached. However, when the screw speed was further increased to much higher speeds, the polymer

degraded due to the heat produced by the mechanical energy of the screws. Therefore, the screw speed needs to be adapted for each purpose, since it has an impact on several factors involved in the extrusion process. If amorphization is targeted, the screw speed would need to be high in order to obtain a high shear mixing with reduced residence time.

1.3 Methods of Characterization

Pivotal to the characterization of hot-melt extrudates is the evaluation of their solid-state (amorphous, crystalline, or partially amorphous) because this in turn influences stability during the product shelf life, crystallization tendency, drug dissolution and drug bioavailability. Evaluation of the solid-state is extremely important to HME since this process promotes the disruption of the crystal lattice and the recovery of an amorphous or partially amorphous solid. (13)

The prepared ASD were characterized for crystallinity using Differential scanning calorimetry (DSC) and X-ray powder diffraction (XRPD). However, in general, these techniques can only be used off-line. Off-line measurements require sampling with careful randomization. Analysis results and information about the quality and properties of the produced drug are obtained with a significant time delay. This is contradictory to the aim of pharmaceutical industries who wish to change their batch processes into continuous manufacturing. (20)

DSC and XRPD have complementary nature. The XRPD is valuable to evaluate the physical structure at room temperature, while DSC can discriminate additional events that occur during heating of the sample and is more sensitive to detect crystalline material than XRPD. The presence of crystalline material reflects itself either in Bragg peaks for XRPD or in a melting endotherm in the case of DSC. Both the position of the Bragg peaks (°2Theta) and the melting point (°C) are characteristic for a specific polymorph. When samples are only partially crystalline, Bragg peaks will be smaller and superimposed on amorphous halos in XRPD, whilst melting endotherms will be smaller for DSC. (21)

1.3.1. Differential scanning calorimetry

In many cases, the thermal stability of a mixture is preliminarily evaluated through thermal techniques, such as DSC. Thermal analysis techniques are based on isothermal, scanning, and modulated temperature. In DSC, a linear or isothermal temperature program is applied as a function of time or temperature simultaneously to a sample and an empty pan (the reference), Fig. 3, making it possible to measure the temperature and the heat flow change associated with state transitions that occur during a specific temperature program in the sample. (13)
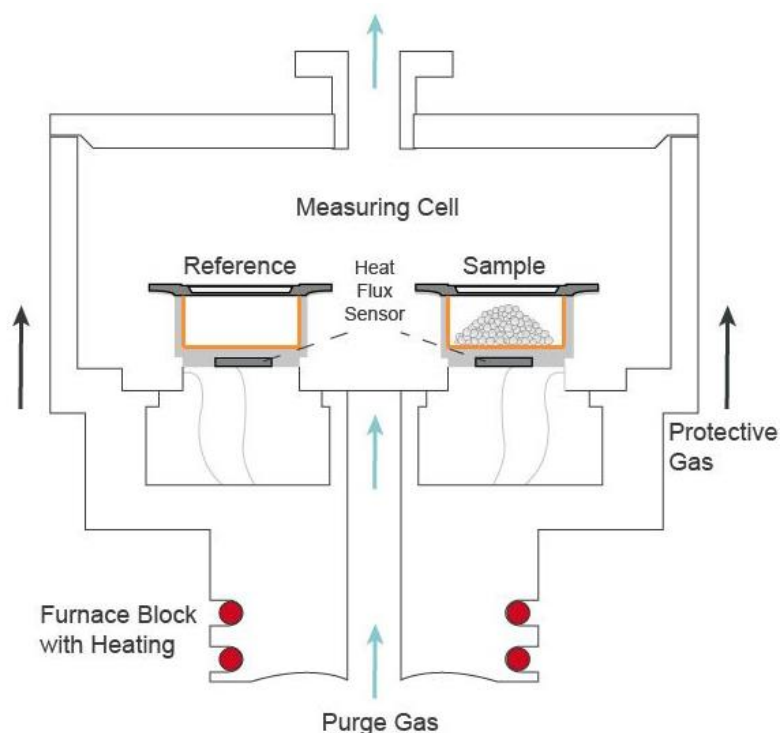
Figure 3. Diagram of a DSC measurement chamber. From (45).

DSC allows for the determination of the glass transition, melting temperatures and weight changes. This results in the identification of the sample thermal stability, degradation and the identification of the optimal temperature interval for the HME process. (13)

The various phase transitions that occur when starch-water mixtures are heated can be monitored using DSC. (22)

Limiting factors of DSC are heat-induced sample alteration, the interfering of residual solvent evaporation with other thermal events and the coinciding of enthalpy recovery with melting events. DSC can also withhold information about the miscibility and the molecular mobility of the system. (21)

Modulated DSC, an evolution of DSC, applies to a sample a sinusoidal (modulated) heating signal on a linear scan (or isothermal) program, thus allowing the separation of the total heat flow response into its reversing (sensible) and non-reversing (latent) components.

TOPEM® mode provides accurate heat capacity values and yields new information not obtained by conventional DSC, which allows the interpretation of different thermal events that occur in the sample. It is a unique multi-frequency technique that allows the separation of superimposed effects. In practice, Modulated DSC can highlight phenomena that otherwise could be masked during heating, for example, a glass transition masked by a desolvation endotherm. (13,23)

1.3.2. X-ray powder diffraction

XRPD is a common technique for the study of structures, phases, preferred crystal orientations (texture), and other structural parameters, such as average grain size, crystallinity and crystal defects. XRPD is a pivotal tool and an indispensable analytical technique supporting a wide variety of pharmaceutical development applications in various stages of drug development and manufacturing. (24)

An X-ray diffractometer (Fig. 4) consists of three basic elements: an X-ray tube, a sample holder, and an X-ray detector.
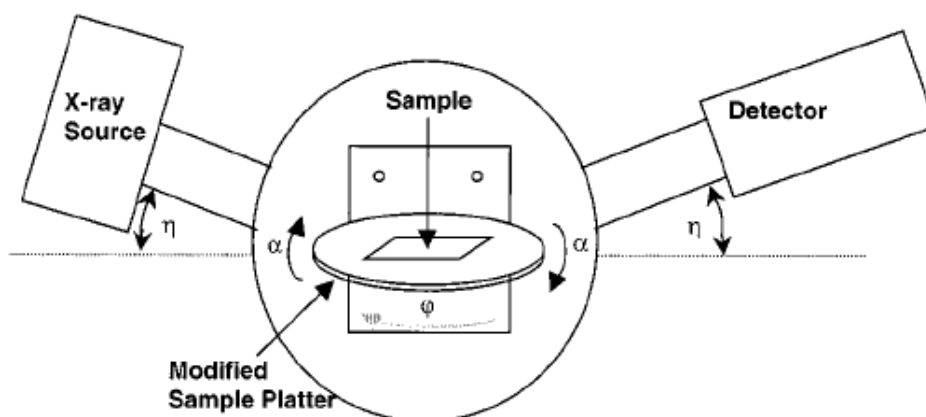
Figure 4. X-ray diffractometer. From (24).

This technique is based on the constructive interference of monochromatic X-rays and a crystalline sample. These X-rays are generated by a cathode ray tube, filtered to produce monochromatic radiation. Copper is the most common target material for single-crystal diffraction. These X-rays are collimated and directed onto the sample. As the sample and detector rotate, the intensity of the reflected X-rays is recorded. When the geometry of the incident X-rays striking the sample satisfies Bragg's law, constructive interference occurs and a peak in intensity appears. The detector records and processes this X-ray signal and converts the signal to a count rate, which is then output to a computer monitor.

The interaction of the incident rays with the sample produces constructive interference (i.e., when the probes are aligned the signal is magnified) and a diffracted ray when conditions satisfy Bragg's law (equation 1):

$$N\lambda = 2dsin\ \theta \quad (1)$$

where **n** is an integer, **λ** is the wavelength of the X-rays, **d** is the interplanar spacing generating the diffraction, and θ is the diffraction angle. (24)

This law relates the wavelength of electromagnetic radiation to the diffraction angle and the lattice spacing in a crystalline sample. X-ray beams hitting crystalline solid materials are scattered in all directions. These diffracted X-rays are then detected, processed, and counted, producing distinct scattering patterns, similar to fingerprints. By scanning the sample through a range of °2θ angles, all possible diffraction directions of the lattice should be attained due to the random orientation of the powdered material. A halo, that is the absence of diffraction peaks, corresponds to a completely amorphous sample. (13,24)

Limiting factors of XRPD are the lack of sensitivity for small traces of crystallinity, the impossibility to differentiate between distinct amorphous phases and its impossibility to detect nanocrystals in a polymer matrix. (21) Moreover, there is the need to ground the material into an extremely fine grained powder to achieve a good signal-to-noise ratio (and avoid fluctuation in intensity), avoid spottiness, and minimize preferred orientation.

This non-destructive technique presents some strengths like the easy sample preparation and the relatively straightforward data interpretation. Regarding the latter, an XRPD pattern is a direct result of the crystal structures that are present in the pharmaceutical under study. XRPD analysis can easily detect the existence of defects in a crystal, its resistance level to stress, its texture, its size and degree of crystallinity, and virtually any other variable relating to the sample's basic structure.

Regarding its applications in the pharmaceutical industry, in the drug design, discovery, development, and formulation process, XRPD can help to establish a formulation by discovering the morphology and the degree of crystallinity, providing unique polymorph identification, and determining the quantity of each in the mixture. XRPD can be used to unambiguously characterize the composition of pharmaceuticals. (24)

1.4 Glass Transition Temperature

The glass transition temperature (T_g), together with the melting temperature (T_m) of both the drug and the polymeric carrier should be considered primarily to the HME process. (16)

The T_g is approximately 2/3 of the melting point (T_m). The "Rule of 2/3" is used to estimate the T_g of a pure amorphous phase based solely on the T_m of the corresponding crystalline phase. T_g is defined as the temperature at which the material transforms from its glassy state to a supercooled liquid state upon heating. The glass transition is a reversible transition in which the material changes drastically its molecular mobility from a solid-like form to a viscous liquid-like form. (25) This process is not a phase change. Unlike T_m, T_g is a kinetic parameter and a useful material descriptor owing to its correlation with structural and thermodynamic properties.

DSC is the principal source of T_g data. The quantitative measurement of T_g considers the scanning rate, annealing (structural relaxation or enthalpy relaxation) and distinguishes between onset, midpoint, and endpoint temperatures. (2,10)

The glass transition temperature can be theoretically predicted from the Gordon-Taylor equation based on the volume additivity of a mixture. Deviation from the predicted values can be explained in terms of immiscibility or with regard to enhanced molecule-molecule interaction. (13)

The addition of small amounts of water to the starch during the extrusion process is necessary for the gelatinization. The T_g of starch depends on water content, which has a very efficient plasticizing effect. (26)

The T_g of starch is one of the critical thermal properties for starch-based products. However, some researchers consider that DSC may not be suitable to study the T_g of starch because the heat capacity of the transition is too weak and frequently is masked by the gelatinization endotherm. Furthermore, the multiple phase transitions that starch undergoes during heating and the instability (such as evaporation) of water contained in starch make it more difficult to study the thermal behaviour of starch using DSC. (27)

1.5   Starch

Starch is one of the most abundant natural polysaccharides of the general formula $(C_6H_{10}O_5)_n$, found on a wide range of crops worldwide. It has been of interest in the paper, pharmaceuticals, cosmetics, thermoplastics and a variety of conventionally processed foods. The primary source of starch is corn, potato, wheat and rice. (26,28) In its native form, pure starch is a white, relatively tasteless powder that is odourless and is insoluble in water and other common organic solvents. (29)

Starch is a mixture of amylose, a linear structure of alpha-1,4 linked glucose units, and amylopectin, a highly branched, tree-like structure of short alpha-1,4-glycosidic chains linked by alpha-1,6 bonds (Fig. 5). Amylose has a molecular weight range of approximately 10^5–10^6,

corresponding to a degree of polymerization (DP) of 1000–10,000 glucose units and amylopectin is a much larger polymer, with a molecular weight about 10^8. (20,26,29,30)

Most native starches are stored as granules and present alternating regions of amorphous and crystalline lamellae seen as rings which are essentially the crystalline portion. A starch granule has a semicrystalline structure with crystallinity variations from 15 to 45%, which is usually transformed in its amorphous state for most applications. Depending on its botanical origin, the amylose/amylopectin ratio can vary: 20/80 for potato starch, 25/75 for normal maize starch, 70/30 for amylomaize (high amylose maize). (20,26,29,30)
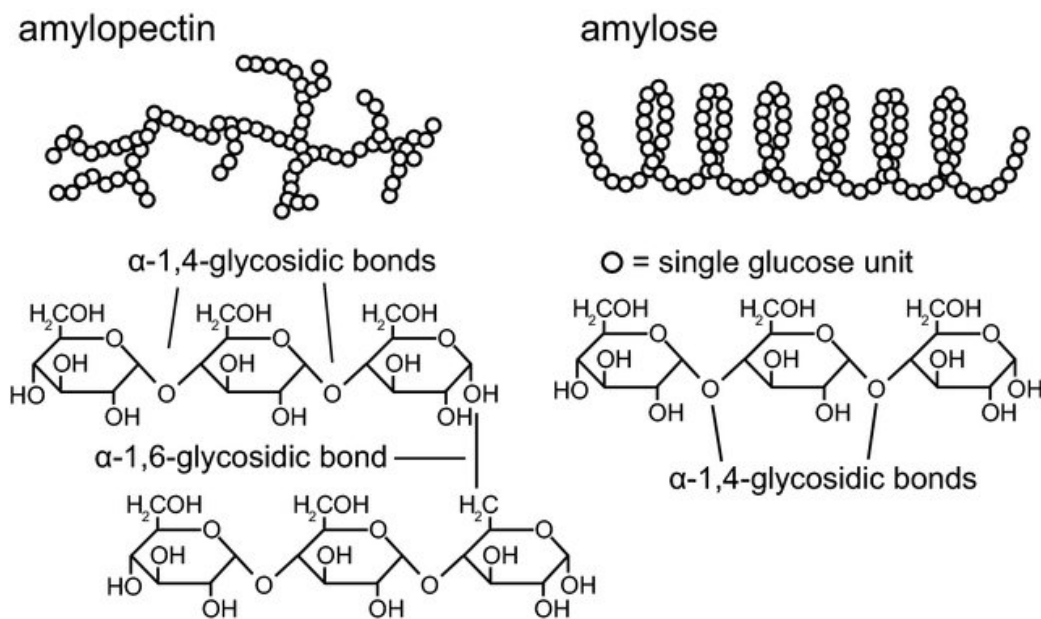
Figure 5. Chemical structure of starch constituting natural polymers, amylopectin and amylose. Amylopectin is a branched polymer, whereas amylose is a linear polymer forming a helix. From (32).

Crystallinity is associated with amylopectin while the amorphous regions are mainly represented by amylose and the branching points of amylopectin. (20,26,29,30) Amylose and amylopectin make up 98–99% of the dry weight of native granules, along with small amounts of lipids, minerals, and phosphorus in the form of phosphates esterified to glucose hydroxyls. The higher the amylose content the more lipid is present in native starches. (31) Moreover, depending on the amylose content, physical properties may vary in melt viscosity, die pressure, and die-swelling at the nozzle. (18)

Gelatinization occurs when native starch is heated in the presence of enough moisture; the granules absorb water, swell and the crystalline organisation is irreversibly disrupted. For most starches, gelatinization occurs in a temperature range between 60 and 80°C. Sufficient moisture must be available for the process of gelatinization to occur. Preparation of gelatinized and modified starches at low water contents has extended shelf-life properties making them relatively inexpensive to handle and transport around the world. Accordingly, they are

successfully incorporated into commercial formulations in the food and pharmaceutical industries, including confectionery products and the hard-gelatine capsule. (22,28) Moreover, starch can act as an absorbent in drug formulations due to its hygroscopic nature, keeping powders dry and ensuring the stability of drugs that are liable to deteriorate by hydrolysis and other similar chemical reactions. (29)

Yet, another key aspect is the issue of recyclability and environmental impact. If possible, only materials that are harmless to the environment should be used and their environmentally friendly disposal must be ensured. (32) The use of natural polysaccharides for the development of drug delivery systems is an interesting alternative to common synthetic polymers. Native and pre-gelatinized starches have been widely used in the pharmaceutical industry as disintegrants, binders, and diluents, due to the properties of biopolymers, making them applicable in pharmaceutical development and biomedical devices. Many publications prove the benefit of hot-melt extruded starch as a matrix former in drug delivery systems, such as transdermal films, implants, pellets, and tablets. (20,26,30,33)

During HME, the starch granules are disrupted and lose their crystalline structure. Since water is a strong plasticizer, the application of heat and water leads to a complete gelatinization of the starch granules. Internal hydrogen bonds are destroyed and replaced by water molecules. Starch melts can be processed by HME at low temperatures (<100°C), which makes them suitable for even thermosensitive APIs. (20,26,30,33)

In its wide use as a pharmaceutical excipient, starch is a safe material. It is worth continuing to explore its applications because of its biocompatible nature.
Advantages of starch use:

- Renewable and eco-friendly
- Inexpensive and widely available natural polymer
- Nontoxic, inflicts nearly no harm on the environment
- Odourless, digestible and biocompatible nature. (20,26,30,33)

Nevertheless, the processing of starch without the addiction of plasticizers often leads to fragile products. (18) There is another limitation to the use of starches in formulation development, which is ensuring batch-to-batch consistency of the different starches produced and harvested in different conditions. It is necessary to make sure the starches from different sources meet compendial standards of quality in the relevant official books (pharmacopeias) and their performance is not dependent on their source or growing conditions. (29)

1.6 Model drugs

1.6.1. Ibuprofen

Ibuprofen (IBU) is a conventional non-steroidal anti-inflammatory drug, which is mainly used for the treatment of mild to moderate pain and fever. IBU is a weak acidic drug with high permeability, which could be absorbed in the stomach after oral administration. The solubility of ibuprofen in the stomach, however, is limited due to the carboxyl group in the chemical structure (Fig. 6). Therefore, increasing the apparent solubility or drug release rate of ibuprofen is essential for its oral bioavailability. (34)
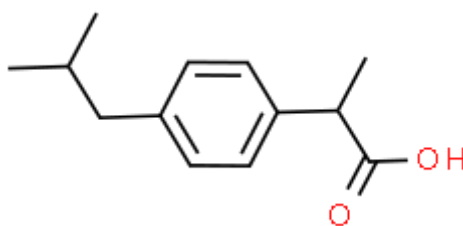
Figure 6. Chemical structure of Ibuprofen. From (46)**.**

The BCS class II compound IBU is often used as a model API as it has been shown to act as a non-traditional plasticizer. IBU presents plasticizing effects compared to traditional plasticizers. Its plasticizing effect can lower the barrel temperature required during the extrusion, which in turn limits degradation. (1,12) IBU is a highly lipophilic molecule and the more lipophilic substances are usually dispersed in the starch matrix. (33)

1.6.2. Carbamazepine

Carbamazepine (CBZ) is an anticonvulsant drug with a structure resembling the tricyclic antidepressants (Fig. 7), which acts as a sodium channel blocker. CBZ is classified as BCS class II due to its low solubility and high permeability (0.15 mg/ml and 4.3×10^{-4} cm/s, respectively). One of the major problems with this API is its very low solubility in biological fluids that results in poor bioavailability after oral administration. (35,36) CBZ is a lipophilic drug (Log P value 2.77) which is poorly water soluble with a slow dissolution rate, hence it shows poor oral bioavailability. (37) The bioavailability of carbamazepine is in the range of 75-85% of an ingested dose. (38) It shows an erratic dissolution profile in the gastric and intestinal fluid due to its poor water solubility. The peak plasma concentration (C_{max}) and the time taken to reach C_{max} (t_{max}) depend upon the extent and rate of dissolution of the drug, respectively. (35)

The equilibrium solubility of drugs is not only dependent on interactions between the drug and solvent but also on intermolecular interactions within the solid-state of the drug. Most drugs are available in their crystalline state, which has strong intermolecular interactions. These

intermolecular interactions lead to strong crystal packing, so they must be disrupted to solubilize the drug. Thus, crystal packing in the solid-state of drugs is a major challenge that affects their solubility. (3,17)
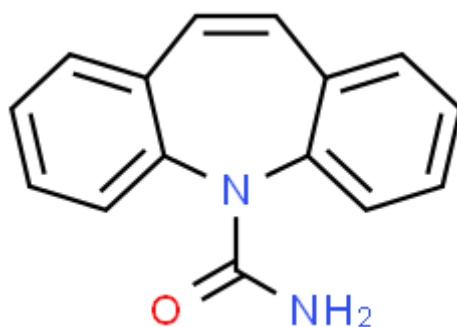

Figure 7. Chemical structure of Carbamazepine. From (37).

APIs can exist in multiple crystalline phases called polymorphs, that have the same chemical composition but different internal structures. Polymorphs exist when the drug substance crystallizes in different crystal packing arrangements, all of which having the same elemental composition. For CBZ, identification and the control of polymorphic transitions are of fundamental importance when assessing the performance of a given formulation. CBZ is known to exist in four polymorphic forms: P-monoclinic (form III), triclinic (form I), trigonal (form II) and a C-monoclinic (form IV), as well as additional pseudo-polymorphic forms, including a dihydrate (DH) form (P-monoclinic), have been hitherto reported in the literature, of which form III is the commercial form. Form I is formed upon exposure to higher temperature, is therefore accessible via tsHME. In this technique, the increase of temperature is not only generated by heat transfer from external sources (barrel heating) into the product, but also from the dissipation of mechanical energy introduced via the twin-screw rotation. (37)

Due to its narrow therapeutic index and relatively high plasma concentration variability, uniform dispersion of CBZ in the dosage form and adequate dissolution rate are very important to achieve the desired therapeutic effect. (3,17)

Table 1. Physicochemical properties of substances under investigation. (1,17,27,33,39)

Substance	Molecular weight (g/mol)	Glass transition temp. (°C)	Melting point (°C)	Water solubility (mg/mL)	LogP	Peak area (cts*2Th)	Hydrogen acceptor count	Hydrogen donnor count
Waxy Starch	-	66	-	-	-	-	-	-
Maize Starch	-	60	-	-	-	-	-	-
Ibuprofen	206	-44	75	0.0684	3.97	13616.0	2	1
Carbamazepine	236	53	175	0.152	2.77	83.38	1	1

2. Aim

2.1 Motivation

The hot-melt extrusion of starches is well known and established in food technologies, however not in the pharmaceutical industry. (40) Concerning synthetic structures, nearly unlimited resources of this natural polysaccharide are available. (18) Therefore, it was of particular interest to evaluate the potential of a natural-based polymer to use as a vehicle for an API in an HME process.

The opportunity to attempt the production of starch-based amorphous solid dispersions (ASD) with BCS-class II drugs came along with the Research Laboratory Exchange, of the Erasmus mobility programme, supervised by Prof. Dr. Karl Wagner of the Department of Pharmaceutical Technology at the University of Bonn, Germany.

This study describes the attempt to produce starch-based ASD with BCS-class II drugs. Considering the need for improved solubility in BCS class II and IV drugs and keeping in mind that the bioavailability of poorly soluble drugs can be increased by incorporation into a water-soluble melt, the APIs used were IBU and CBZ. The main challenge was the preparation of solid dispersions (SD) using a natural polymer such as starch. The SD were produced using two different types of starch in a co-rotating twin-screw extruder.

2.2 Overall goals

The present study aims to produce an ASD using a widely available natural-based polymer, to provide a better insight into the HME process, the characterization methods and further understanding of the thermodynamic behaviour of hot-melt extruded starches with incorporated APIs.

The present study has three main goals:

a) The first objective set to be achieved is to evaluate the influence of the extrusion parameters on the amorphization of the extrudates using a diffractometry technique, XRPD.

b) The second is to get a detailed insight into the thermal behaviour of a starch-API system using a calorimetry tool, DSC.

c) The third one is the thermophysical characterization of the solid-state of starch-based extrudates, manufactured via HME.

To achieve these goals the first task established was the attempt to manufacture ASD using only starch, an API and water to allow gelatinization. This task required the optimization of the extrusion parameters through several extrusion runs to produce an ASD.

APIs and polymers for evaluation should be selected based upon API-polymer physicochemical properties such as solubility parameters, hydrogen bonding, and thermal properties.

Two different starch types, maize corn starch (MS) and waxy corn starch (WS), chosen as the polymer matrix, with two different APIs, IBU and CBZ, were extruded. Extrusion temperatures were selected based on the materials melting points and glass transition temperatures.

Finally, the extruded samples of MS and WS with IBU and CBZ were characterized and XRPD was used to determine the solid-state of the drug in the formulations after processing.

3. Materials and Methods

3.1 Materials

Ibuprofen (IBU) and Carbamazepine (CBZ) were provided by BASF SE (Ludwigshafen, Germany). The APIs were chosen due to their various physicochemical characteristics.

Maize Starch (MS) and Waxy Starch (WS) (Waxilys®200) were obtained from Roquette (Lestrem, France), with different ratios of amylose and amylopectin.

3.2 Preparation of physical mixtures

The physical mixtures were mixed for 5 min at 50 rpm in a powder tumble blender (Turbula Type T2A, Willy A. Bachofen, Basel Switzerland).

Before the HME tests, DSC was used to assess the T_g of both MW and WS and to identify the temperature interval for the HME process. The extrusion temperature should be higher than the T_g and never reach values >100 °C.

The search for a better API for starch-based ASD was performed. It was considered and compared the T_g, T_m, water solubility, donor/acceptor groups of H-bonds, LogP of the starches and several candidate APIs for further HME tests. The rule "*Similia similibus solvuntur*" ("like dissolves like") applies, i.e., two materials with similar solubility parameters are expected to be miscible. (5) Hence, by comparing both APIs physical properties, CBZ was then extruded along with the starch matrix, replacing IBU as the API.

3.3 HME – Process of Manufacturing

The physical mixture was dosed into the extruder by a volumetric feeder system ZD9 (Three-Tec GmbH, Seon, Switzerland). The feed rate of each mixture into the extruder had to be adapted according to the rheological properties of each composition, to have 2 g of the physical mixture entering the extruder barrel per minute.

The HME was performed using a co-rotating twin-screw extruder ZE12 (Three-Tec GmbH, Seon, Switzerland) with a functional length to diameter ratio of 25:1, screw diameter of 12 mm and a maximum torque of 15 N·m. Process temperature was at a maximum in the high-shear zone of the screws (kneading elements of 30° and 60° angle (green area)), 60° and 90° 4disc-kneading elements (red and green area). The screw configuration is shown in Fig. 8. The twin screws rotate together and are fully intermeshing.

The extruder barrel consisted of five individually adjustable heating zones, enabling complete melting and an even distribution of the API. The temperature was reduced at the

terminal zone of the barrel to initiate the solidification of the material. The screw speed varied from 100 to 300 rpm, the latter being the maximum allowed by the extruder.

To humidify the mixture, water was simultaneously fed into the extruder with an HPLC pump.
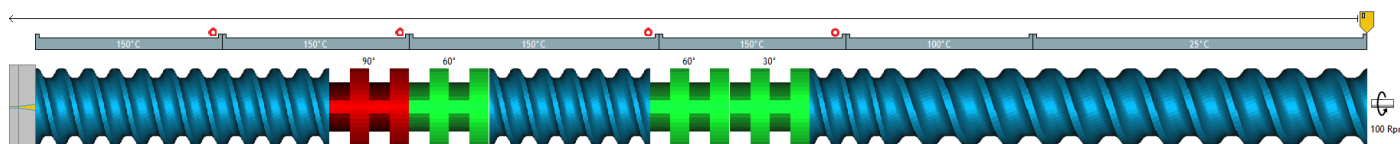

Figure 8. Extruder and screw configuration used. (Blue areas = conveying elements; Red and Green areas = kneading elements). Screenshot from the simulation software Ludovic® V6.2.1 PharmaEdition (Sciences Computers Consultants, Saint Etienne, France).

3.3.1. Extrusion process parameters

The starch-based extrudates were prepared using different temperature profiles (Table 2). The extrusion temperatures ranged from 40 °C at the inlet to a maximum 100 °C at the die of the extruder. The rotational speed of the screw was adjusted to 100 rpm initially for all tests.

To evaluate the influence of the extrusion parameters on the amorphization of the extrudates, two different starch PM with IBU were extruded with two different moisture contents, 15% and 20% water content, which corresponds to 0.3 ml/min and 0.4 ml/min, respectively. These values mean that 0.3/0.4 ml of water was being fed to 2 g of the physical mixture entering the extruder barrel, per minute.

Table 2. Extrusion conditions for the production of hot-melt extruded products.

Extrusion	Starch	API	API (% w/w)	PM dosing (g/min)	Water content (ml/min)	Rotation Speed (rpm)	Heating zone Temperature (°C)				
							1	2	3	4	5
A1	Waxy	IBU	10	2	0.4	100	40	60	85	75	50
A2			20	2	0.4	100	40	60	85	75	50
AM1	Maize	IBU	10	2	0.4	100	40	60	85	75	50
AM2			20	2	0.4	100	40	60	85	75	50
B1	Waxy	IBU	10	2	0.3	100	60	80	90	80	60
B2			20	2	0.3	100	60	80	90	80	60
BM1	Maize	IBU	10	2	0.3	100	60	80	90	80	60
BM2			20	2	0.3	100	60	80	90	80	60
C1	Waxy	IBU	10	2	0.3	100	60	90	100	90	70
C2			20	2	0.3	100	60	90	100	90	70

On a subsequent HME test, a mixture of WS containing 10% w/w of CBZ was used for the preparation of solid dispersions by the HME process. A 10% drug loading level of CBZ in MS was also selected for investigation (Table 3).

Table 3. Extrusion conditions for the production of hot-melt extruded products.

Extrusion	Starch	API	API (% w/w)	PM dosing (g/min)	Water content (ml/min)	Rotation Speed (rpm)	Heating zone Temperature (∘C)				
							1	2	3	4	5
D0	Waxy	-	-	2	0.4	100	60	85	95	80	70
				2	0.4	200	60	85	95	80	70
D15	Waxy	IBU	10	2	0.3	100	60	85	95	80	70
			10	2	0.3	200	60	85	95	80	70
			10	2	0.3	300	60	85	95	80	70
D20	Waxy	IBU	10	2	0.4	100	60	85	95	80	70
			10	2	0.4	200	60	85	95	80	70
			10	2	0.4	300	60	85	95	80	70
DCW	Waxy	CBZ	10	2	0.4	100	60	85	95	80	70
			10	2	0.4	200	60	85	95	80	70
			10	2	0.4	300	60	85	95	80	70
DCM	Maize	CBZ	10	2	0.4	100	60	85	95	80	70
			10	2	0.4	200	60	85	95	80	70
			10	2	0.4	300	60	85	95	80	70

The extrudates were collected 10 min after a homogeneous extrudate strand with stabilized extrusion conditions was observed coming out of the round-shaped die.

3.4 Thermogravimetry

For determining the residual moisture of the extruded products, a thermogravimetric analyzer (TGA 7) from Perkin Elmer (Überlingen, Germany) was used. The sample mass was about 5-6 mg. The atmosphere was held isothermal at 60°C for 1 min, followed by a temperature scan from 60 to 300°C. The heating rate was set to 10°C /min.

3.5 Sample treatment

3.5.1. Drying

The samples were put in a drying oven (Memmert U40, Schwabach, Germany) at 40°C for ±12h, to remove the water added during the extrusion process.

3.5.2. Grinding method

Grinding is accomplished either through hand grinding or in a mechanical grinder. This should be done with great caution as excessive grinding can easily break down the particle size to nanometer size and lead to amorphization. The effects of excessive grinding include lattice distortion and the possible formation of an amorphous layer (Beilby layer) at the surface of the grains. (24)

All extruded products were ground to form powdered material that was used for analyses. For the extruded products manufactured by the conditions displayed in Table 2, grinding was accomplished through hand grinding.

A ball mill (MM 400, Retsch, Haan, Germany) was used to grind the extrudates produced according to the extrusion parameters in Table 3. The grinding jar was filled with the metal grinding ball and with a volume of approximately 10 ml of extrudate. Grinding was performed for 15 s at a frequency of 30.0 Hz, to form a fine powder. Beware of the possibility that the ball mill might have been a source of amorphization to the samples, interfering with the subsequent analyzes.

3.6 Characterization methods

The ground extrudates were analysed by XRPD and DSC.

3.6.1. X-ray powder diffraction

XRPD measurements of the extrudates produced according to the parameters of Table 2 were performed in reflection mode (X'Pert MRD Pro, PANalytical, Almelo, Netherlands) with an X'Celerator detector and nickel filtered CuKα1 radiation (λ=1.5406Å) at 45 kV and 40 mA. Scans were performed at a diffraction angle ranging from 5° to 35° 2Θ with a scanning rate of 0.04°/s and a resolution of 0.001°. The samples were scanned with circular sample holders made of stainless steel.

The extrudates produced according to the conditions of Table 3 were analysed using the transmission mode. Transmission geometry for X-ray diffraction is a more recent method to analyse samples which pose problems in the traditional reflection mode geometry. These can

include organic materials such as pharmaceuticals, proteins, polymers, powders prone to preferred orientation effects such as needles or platelets, liquid dispersions, air sensitive or hazardous materials, and samples requiring low angle diffraction, such as clays or mesoporous materials. X-ray analytical techniques that make use of a transmission geometry require samples that are sufficiently transparent for the type of X-rays used. Sample preparation for experiments can be done via confinement e.g. between thin polymer foils or in a capillary, or as free-standing objects. Additionally, this method requires a smaller amount of sample. (41) The evaluation was carried out by using X'Pert HighScore Plus software from PANalytical (Almelo, Netherlands).

3.6.2. Differential scanning calorimetry

The solid-state analysis as well as the glass transition temperature were evaluated by a DSC 2 (Mettler Toledo, Gießen, Germany) equipped with an autosampler, nitrogen cooling and nitrogen as purge gas (30ml/min) was used. The system was calibrated with n-octane, indium and zinc standards.

For the measurement of the neat starches T_g, approximately 25 mg of neat starch with 20 µL of deionized water were weighed in 50 mg aluminium pans, which were then sealed to allow gelatinization. An empty aluminium pan was used as a reference.

The neat starches were measured in TOPEM® mode (modulated DSC). The thermal transition parameters [onset (T_o), peak (T_p) and endset (T_e) temperatures] were determined from the data recording STARe software.

Approximately 7-10 mg of extrudate were weighed accurately and sealed in 50 mg aluminium pans with a pierced lid. A heating ramp at a rate of 2K/min was then applied. All measurements were performed in duplicate.

4. Results and Discussion

4.1. Effect of HME processing conditions

During the extrusion, the viscosity of the molten system, which must be controlled to enable the flow through the die, was a challenge to keep constant. In this project, Ibuprofen was chosen for its plasticizing properties.

On several extrusion runs the die would get clogged due to insufficient water supply or because of dried starch clogged at the die opening. As a consequence, the torque went up to critical levels to the point where it was necessary the addition of a substantial amount of water to stabilize it and reinitiate the run.

The extrudates were evaluated visually. Most samples exhibited a white opaque homogeneous colour, characteristic of a crystalline material.

The IBU extruded filaments were not clear and translucent but opaque and white. The gelatinized starch matrix can solve a limited amount of API. When the saturation limit is exceeded, the colour of the extrudate strands changes into a persistent white. Therefore, it is possible to say we produced a saturated IBU-starch solution in which ibuprofen was dispersed in the crystalline form.

A specific form of melt flow instabilities associated with surface defects for polymer extrudates, and commonly referred to as the "sharkskin effect" appeared on the IBU extrudates with less water. When this effect occurs, a regular pattern of ridges on the surface is observed resembling the skin of a shark if bent (Appendix 1 (a) and (b)).

At higher temperatures than 90 °C, the extrudate strands with CBZ exiting the die were viscous, exhibited bubble-like areas and a greyish colour (Appendix 1 (c)). It is also visible the die swell phenomenon, which occurs when the material leaves the die and its shape gets deformed because entropy is maximized and it undergoes stress relaxation (Appendix 1 (c)).

4.2. X-ray powder diffraction

Prior to extrusion, the neat starches diffractograms evidence a semi-crystalline material, characterized by an amorphous contribution zone and several absorption peaks (Fig. 9). Both the Maize Corn Starch and the Waxy Corn Starch exhibit an A-type pattern, with characteristic X-ray diffraction peaks at 15, 17, 18 and 23° (2θ). The observed patterns agree with the results obtained by Kipping et al. (30) and Liu et al. (22).
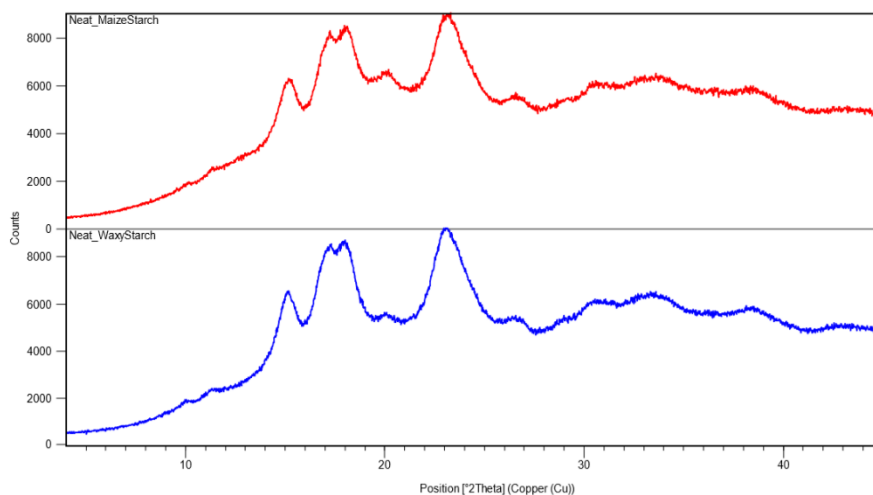
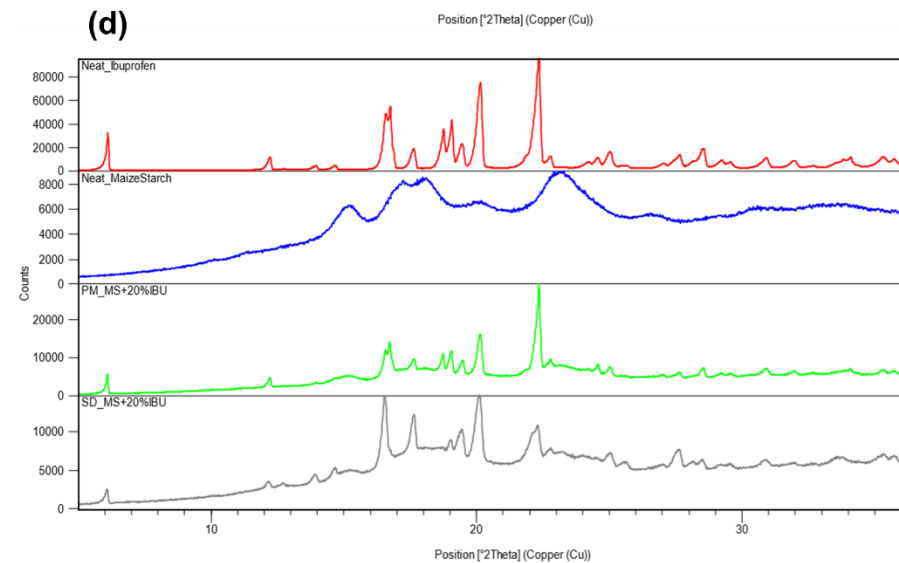**Figure 9. X-ray diffraction patterns of neat Maize Starch (red) and neat Waxy Starch (blue).**

4.2.1. Degree of crystallinity

The degree of crystalline content is a crucial parameter. The amount of crystallinity has a sizeable impact on the stability and performance of a pharmaceutical product. Therefore, it is important to characterize each product in this matter.

The relative crystallinity is defined as the ratio of the peak area of the highest peak to the total area of a diffractogram (which is the sum of peak areas and amorphous areas) of the pure API, in this case, expressed as a percentage.

Table 4. Relative crystallinity of the IBU+WS physical mixtures (PM) and solid dispersions (SD).

| Material	Peak area (cts*°2Th)	Relative crystallinity (%)
Neat IBU	13616.00	100.0
PM 10%IBU+WS	2513.98	100.0
PM 20%IBU+WS	4520.21	100.0
SD A 10%IBU+WS	1062.57	42.3
SD A 20%IBU+WS	2315.08	51.2
SD B 10%IBU+WS	994.67	39.6
SD B 20%IBU+WS	2248.96	49.8
SD C 10%IBU+WS	856.58	34.1
SD C 20%IBU+WS	2561.36	56.7
PM 10%IBU+MS	1785.97	100.0
PM 20%IBU+MS	2302.38	100.0
SD A 10%IBU+MS	1011.76	56.7
SD A 20%IBU+MS	1939.28	84.2
SD B 10%IBU+MS	825.41	46.2
SD B 20%IBU+MS	2412.62	
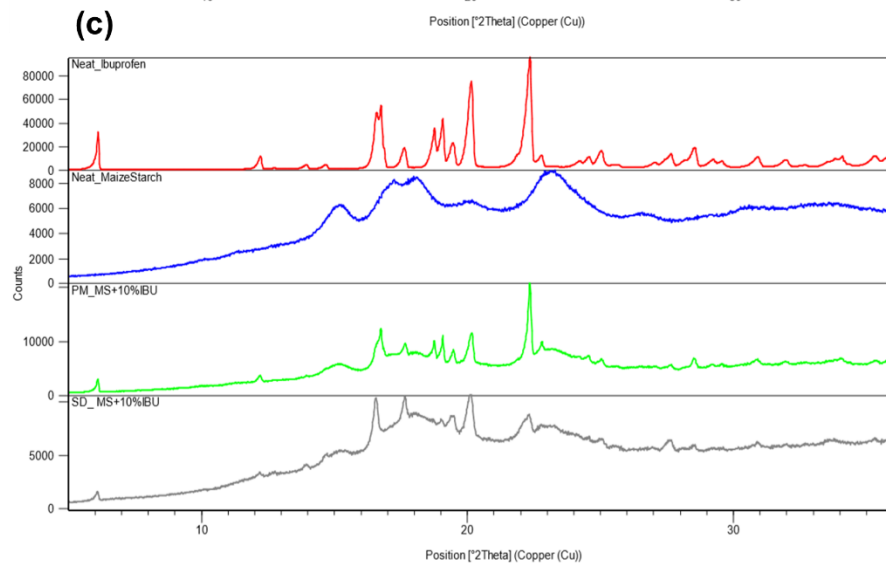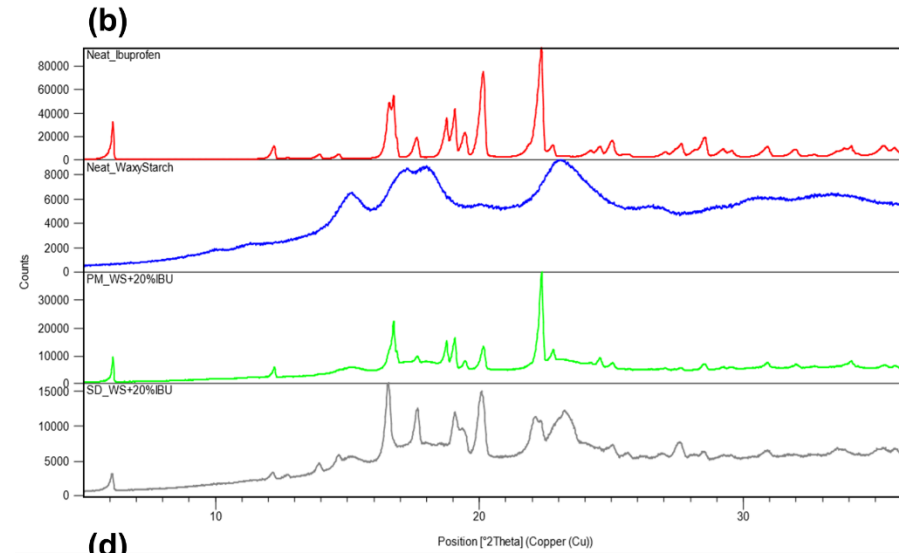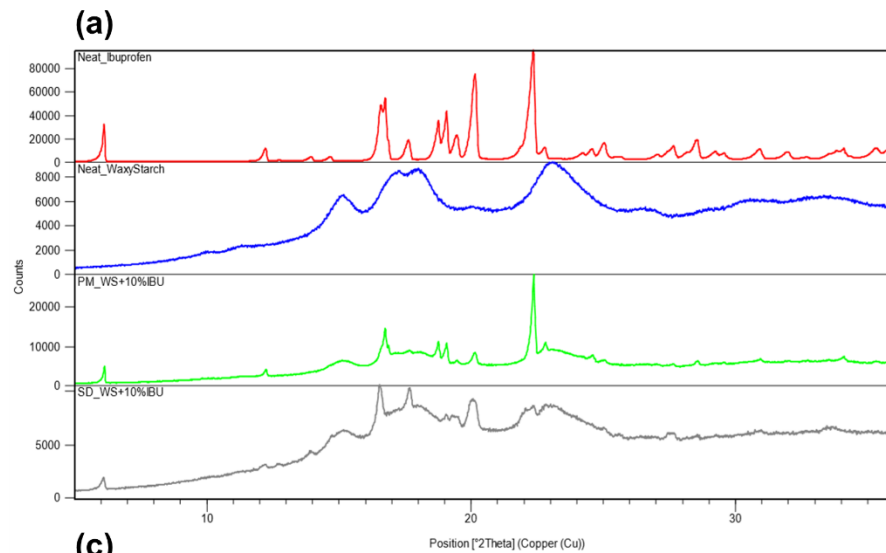
Figure 10. X-ray diffraction patterns of: (a) neat Ibuprofen (red), neat Waxy Starch (blue), A1 physical mixture (green) and A1 solid dispersion (grey) (b) neat Ibuprofen (red), neat Waxy Starch (blue), A2 physical mixture (green) and A2 solid dispersion (grey (c) neat Ibuprofen (red), neat Maize Starch (blue), AM1 physical mixture (green) and AM1 solid dispersion (grey) (d) neat Ibuprofen (red), neat Maize Starch (blue), AM2 physical mixture (green) and AM2 solid dispersion (grey).
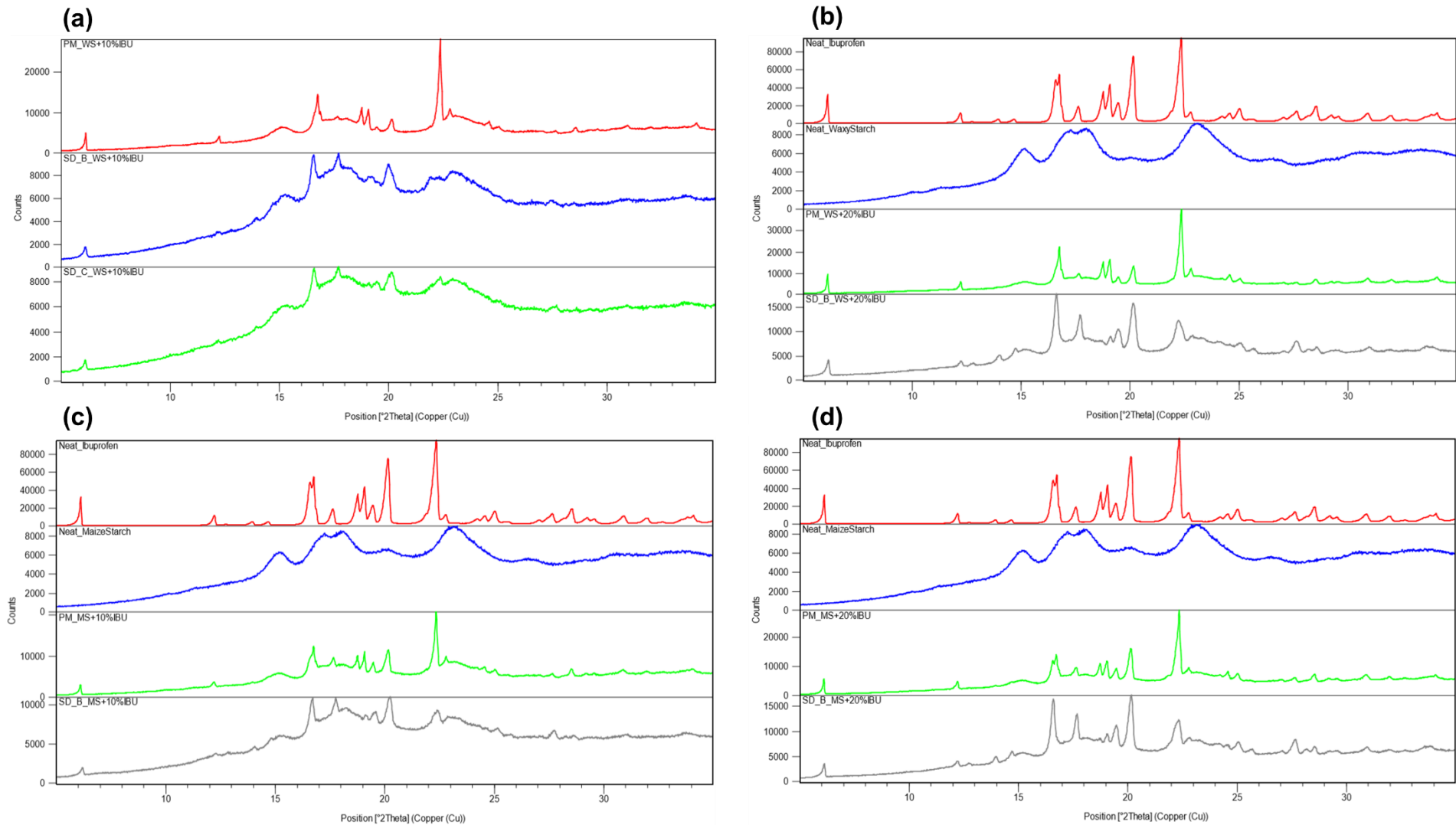
Figure 11. X-ray diffraction patterns of: (a) 10%IBU+Waxy Starch physical mixture (red), B1 solid dispersion (blue), C1 solid dispersion (green) (b) neat Ibuprofen (red), neat Waxy Starch (blue), B2 physical mixture (green) and B2 solid dispersion (grey) (c) neat Ibuprofen (red), neat Maize Starch (blue), BM1 physical mixture (green) and BM1 solid dispersion (grey) (d) neat Ibuprofen (red), neat Maize Starch (blue), BM2 physical mixture (green) and BM2 solid dispersion (grey).
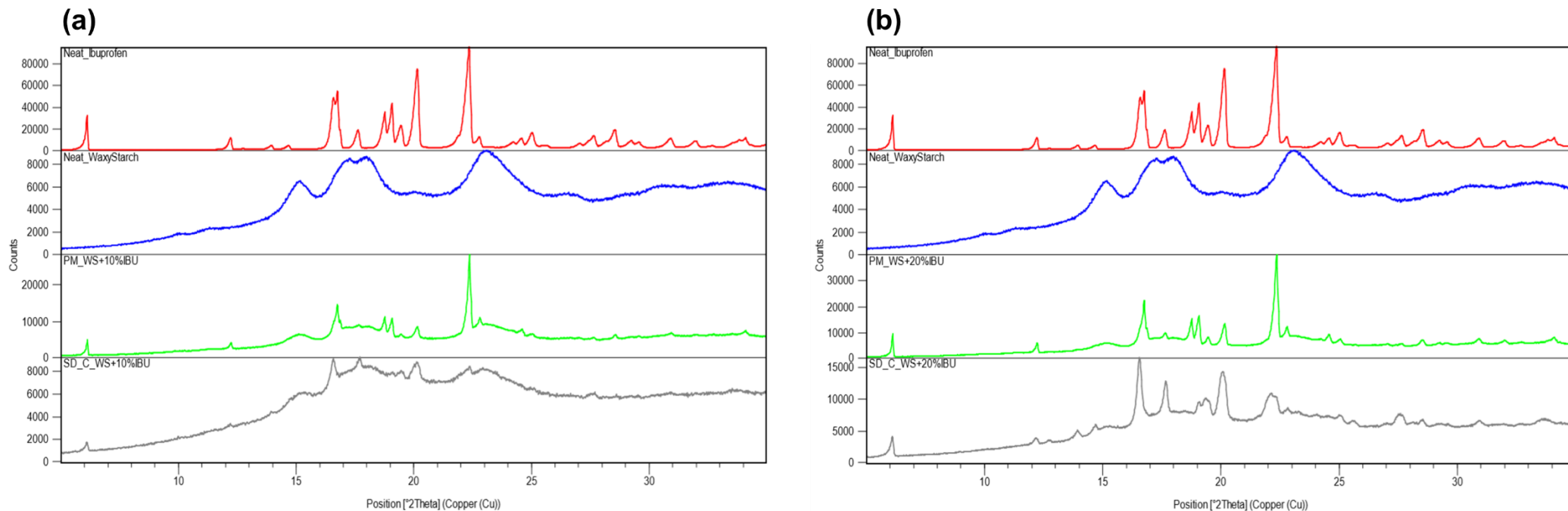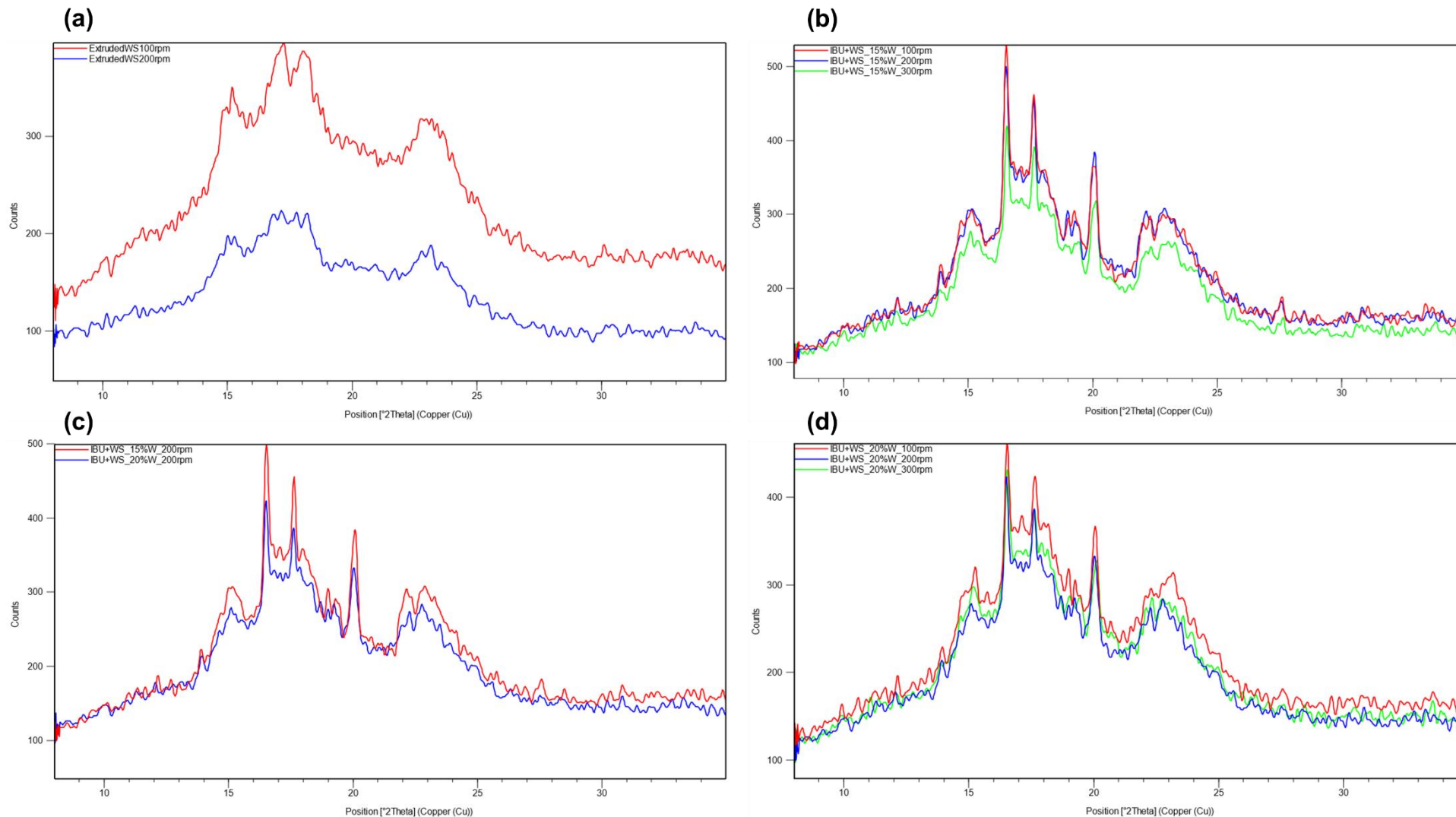
Figure 12. X-ray diffraction patterns of: (a) neat Ibuprofen (red), neat Waxy Starch (blue), C1 physical mixture (green) and C1 solid dispersion (grey) (b) neat Ibuprofen (red), neat Waxy Starch (blue), C2 physical mixture (green) and C2 solid dispersion (grey).

The following diffractograms were produced using the transmission mode.

A smoothed curve was plotted under the raw curve.

Figure 13. X -ray diffraction patterns of extruded neat Waxy Starch at 100 rpm (red) and 200 rpm (blue) (b) X-ray diffraction patterns of D15 solid dispersions at 100 rpm (red), 200 rpm (blue) and 300 rpm (green) (c) X-ray diffraction patterns of D15 (red) and D20 (blue) solid dispersions at 200 rpm (d) X-ray diffraction patterns of D20 hot-melt extruded products at 100 rpm (red), 200 rpm (blue) and 300 rpm (green).

4.2.2. Influence of water addiction

Extrusion runs with 15% and 20% water were performed. Water as a strong plasticizer decreases the viscosity of the melt. The residual moisture content of the extruded products was analysed. The results revealed that extrudates with higher % m/m of API had a slight decrease in water content, 17.8% water in A1 SD and 16.7% water in A2 SD.

According to Kipping et al. (30), the decrease in moisture content seems to be related to water distribution in starch, which is preferential in crystalline regions. The formation of crystal unit cells with low packaging density can lead to entrapment of water.

The XRPD patterns of D15 and D20 SD in Fig. 13 (c) allow the comparison between using 15% or 20% water. Amorphization seems to be favoured with 20% water (blue pattern).

4.2.3. Physical characterization of IBU SD

XRPD was used to confirm the state of IBU in its starch-based SD. The intense peaks, which could be observed from the spectra of IBU bulk powder, indicated that IBU existed as a crystalline compound. As can be seen from Figs. 10-12 and confirmed by Gryczke et al. (42), the characteristic IBU intensity peaks could be identified at 6.03°, 12.09°, 16.48°, 17.55°, 18.75°, 20.02°, 22.13°, 24.47°, 24.99°2θ.

The characteristic diffraction peaks of pure IBU powder also appeared in the diffractograms of IBU solid dispersions, which agreed with the DSC measurements. The evaluation of the XRPD profiles of all starch samples containing IBU shows that crystalline contribution on the profile of the SD is fundamentally due to the presence of IBU. Therefore, it can be assumed that IBU was embedded in the starch matrix in its crystalline form. This behaviour is characteristic of a SD formulation.

As displayed in Fig. 13 (a), (b), and (d), the X-ray diffraction patterns of extruded neat Waxy Starch, D15 and D20 solid dispersions at different rpm. It is possible to claim the screws rotation speed has an impact on the amorphization of starch and IBU, revealing a more amorphous extrudate at a higher rpm value since the 300 rpm green pattern line (Fig. 13 (b)) stands below the other two lines, having a smaller intensity in counts value.

(a)

(b)
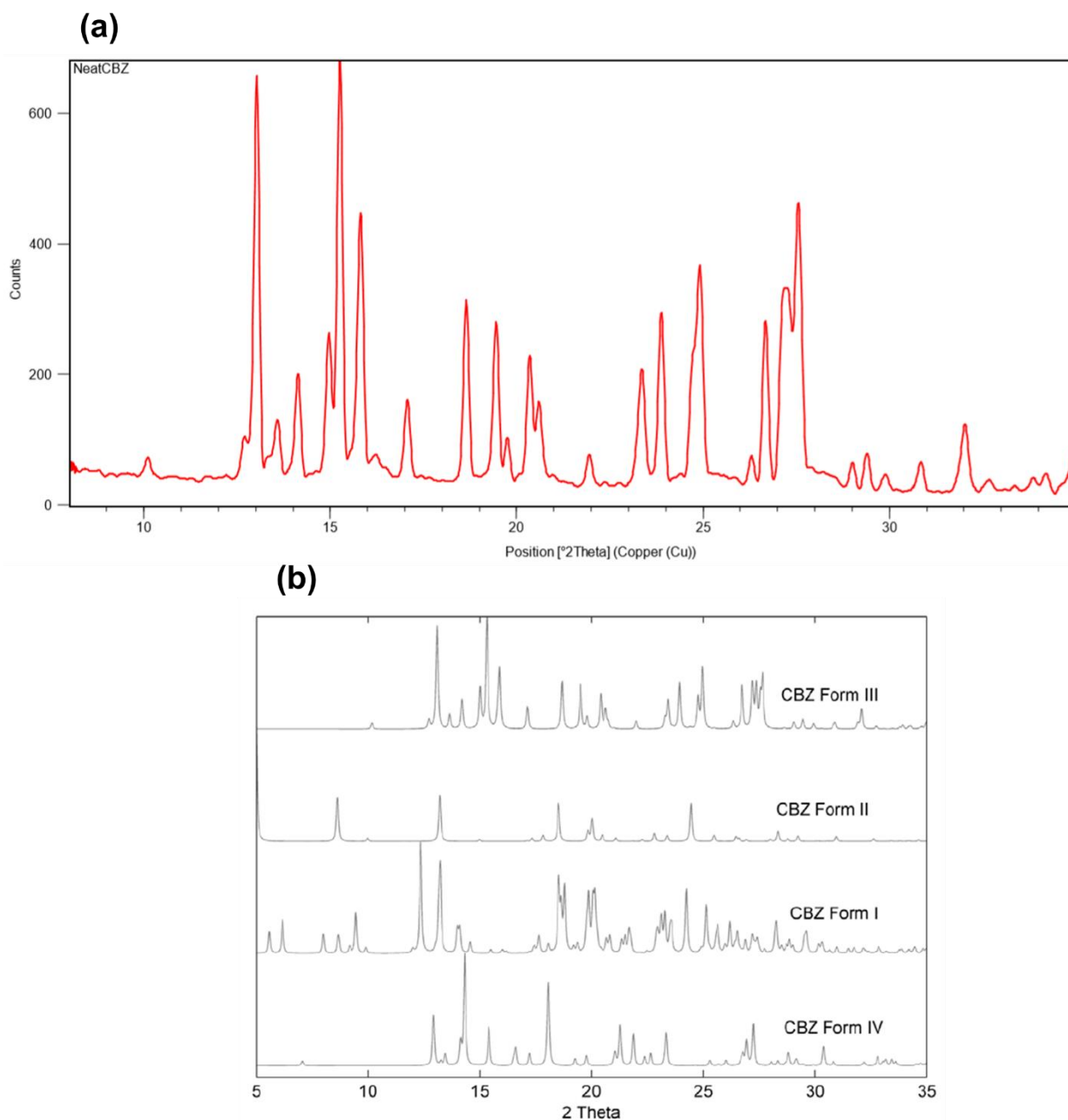
Figure 14. (a) X-ray diffraction pattern of neat Carbamazepine
(b) XRPD patterns of four carbamazepine polymorphs. From (43).

According to Malwade et al. (43) and Steffens et al. (44), in XRPD the CBZ polymorph form I generates major peaks at 8.0, 9.4,12.3 and 20.0°2θ. The CBZ form II shows characteristic peaks at 5.0, 8.7, and 24.4°2θ instead, whereas signal characteristics for form III are found at 13.1, 15.3 and 27.5°2θ. The form DH exhibits two pronounced peaks at 9.0° and 12.4°2θ and a strong signal at 19.5°2θ.

The diffractogram of the neat CBZ in Fig. 14 (a) matches the characteristic signals of form III. The XRPD patterns from the solved crystal structures of four polymorphs of CBZ obtained from Cambridge Crystal Structure Database are shown in Fig. 14 (b).
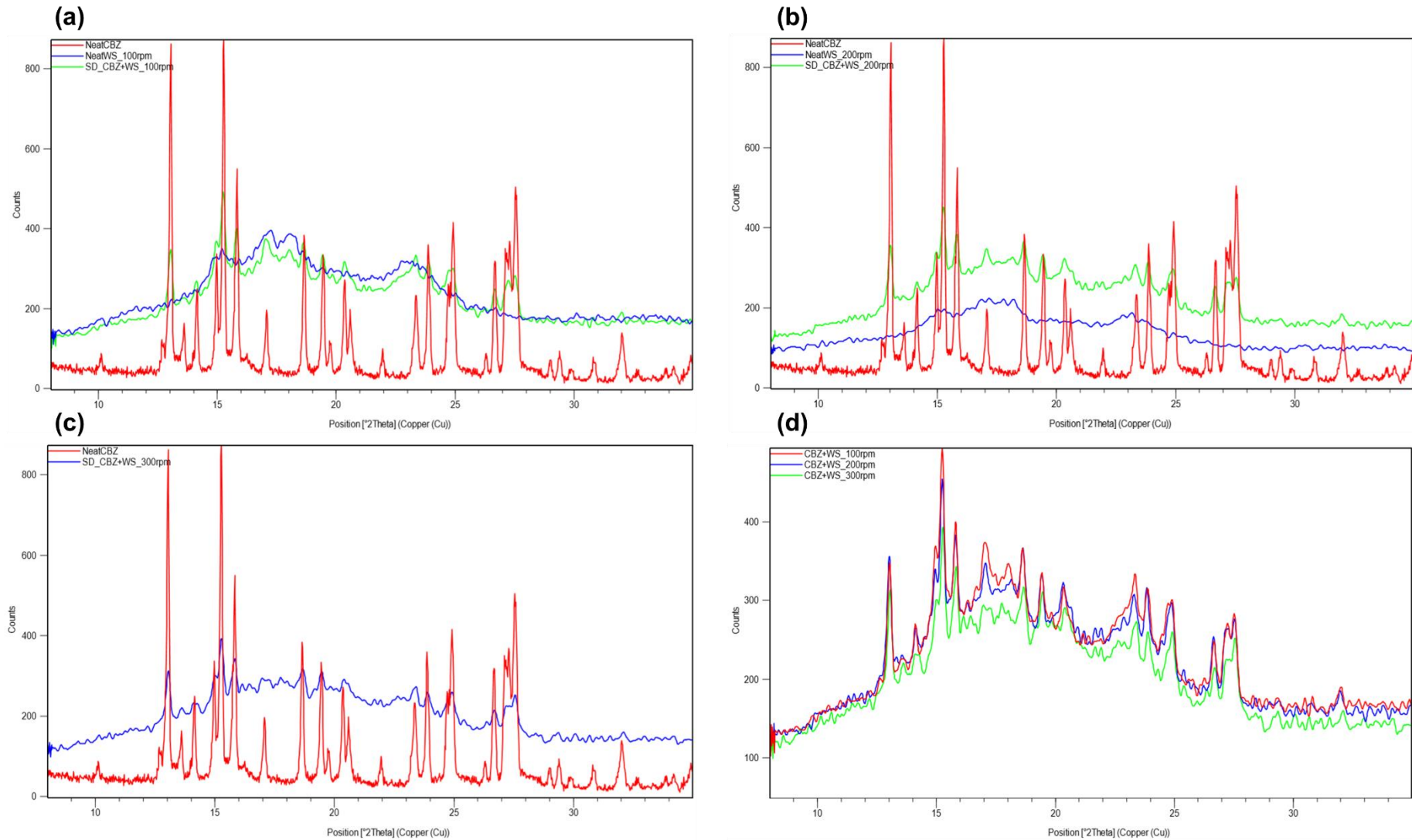
Figure 15. X-ray diffraction patterns of: (a) neat Carbamazepine (red), neat extruded Waxy Starch (blue) and DCW solid dispersion (green) at 100 rpm (b) neat Carbamazepine (red), neat extruded Waxy Starch (blue) and DCW solid dispersion (green) at 200 rpm (c) extrusion DCW hot-melt extruded products at 300 rpm (d) DCW hot-melt extruded products at 100 rpm (red), 200 rpm (blue) and 300 rpm (green).
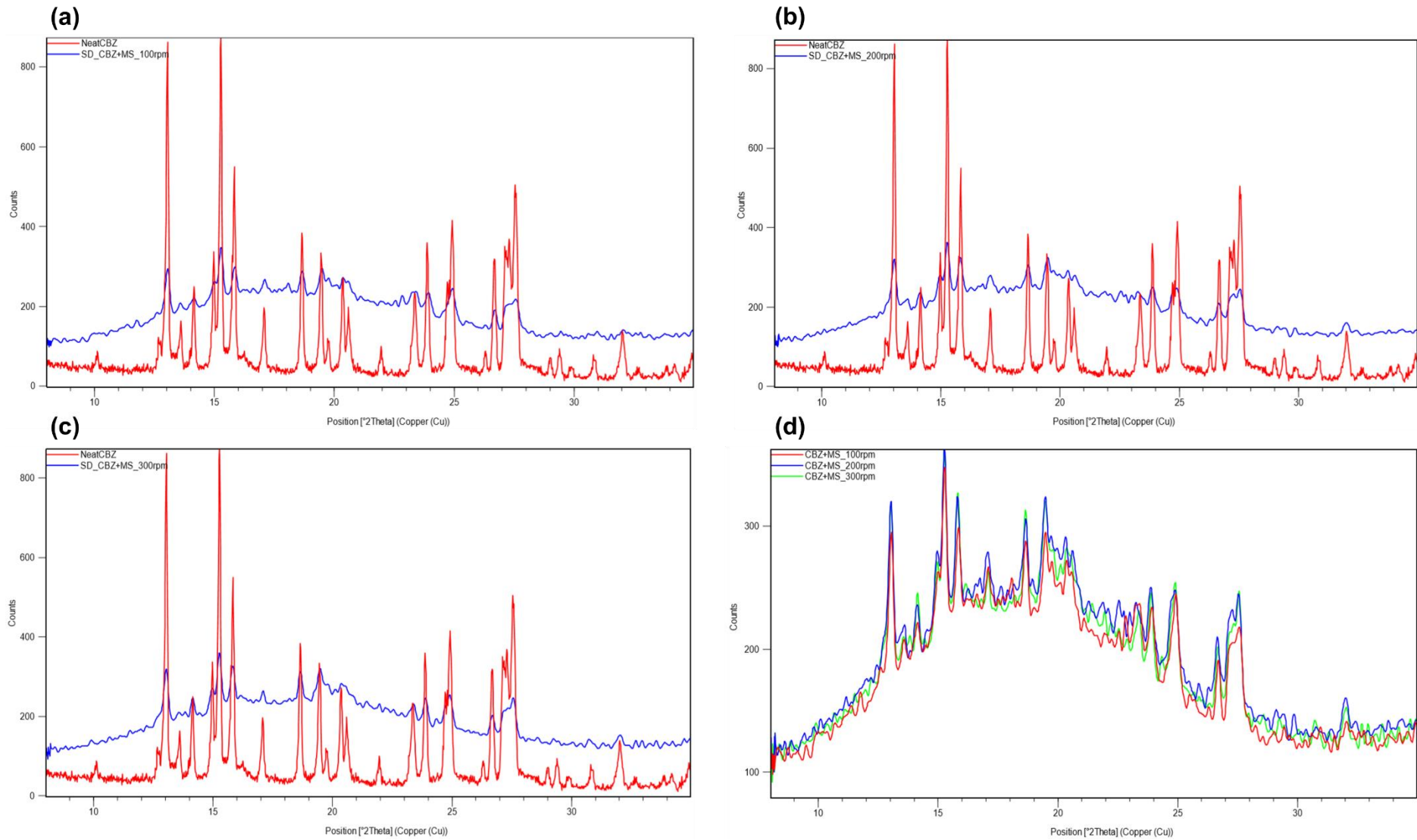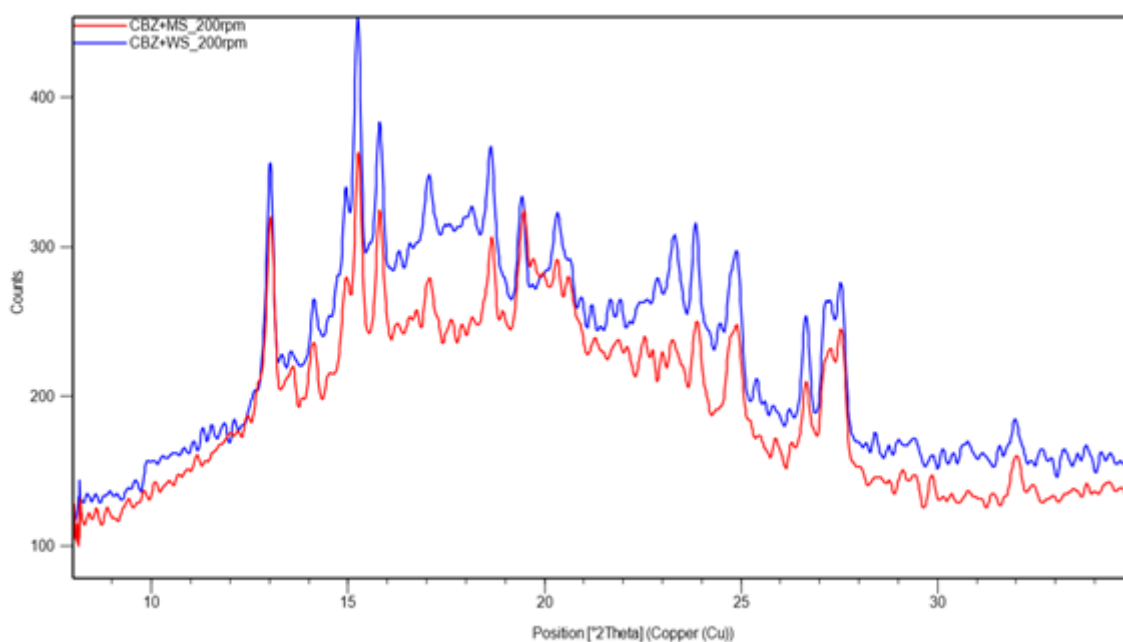
Figure 16. X-ray diffraction pattern of: (a) extrusion DCM hot-melt extruded products at 100 rpm (b) extrusion DCM hot-melt extruded products at 200 rpm (c) extrusion DCM hot-melt extruded products at 300 rpm (d) DCM hot-melt extruded products at 100 rpm (red), 200 rpm (blue) and 300 rpm (green).

46

Relative crystallinity was quantitatively determined by integrating the area under the curve, then relating the area of the crystalline regions to the total diffraction area.

Table 5. Relative crystallinity of the CBZ physical mixtures (PM) and solid dispersions (SD).

Material	Peak area (cts*°2Th)	Relative crystallinity (%)
Neat CBZ	83.38	100.0
SD DCW 100 rpm	75.14	90.1
SD DCW 200 rpm	22.94	27.5
SD DCW 300 rpm	26.25	31.5
SD DCM 100 rpm	28.84	34.6
SD DCM 200 rpm	13.86	16.6
SD DCM 300 rpm	23.18	27.8

Figure 17. X-ray diffraction patterns of the CBZ solid dispersions with Maize Starch (red) and Waxy Starch (blue) at 200 rpm.

As displayed in Fig. 17, Waxy starch, an amylose-free starch, reveals itself to be more crystalline, which agrees with several authors. According to Copeland, Blazek, Salman, & Tang (31) the extent of crystallinity of native starch granules ranges from about 15% for high-amylose starches to about 45–50% for waxy starches.

4.2.4. Physical characterization of CBZ SD

The overall intensity of CBZ peaks was decreasing with increasing polymer content, as expected, due to the amorphous nature of the polymer.

As displayed in Fig. 15 (d), the X-ray diffraction profile of CBZ-WS SD at different rotations, it is possible to claim the screws speed has an impact on the amorphization of starch and CBZ, revealing a more amorphous extrudate at a higher rpm value since the 300 rpm green pattern line stands below the other two lines, having a smaller intensity in counts value.

4.3. Differential scanning calorimetry

For the evaluation of the neat starches diffractograms on the TOPEM® mode (modulated DSC) of the STARe software, the reversing heat flow was selected, and the curve was integrated.

The step in the curve corresponds to the glass transition temperature and is caused by the change in heat capacity of the sample (Fig. 18 and 19). The size of the step in the curve represents the amount of the amorphous material in the sample. The T_g is a measure of the ability of the molecules to move. If there is a shift to the left, to a lower temperature, it means it is easier for the molecules to move. A higher T_g represents lesser molecular mobility.

All the samples analysed were thermally characterized by one single endothermic peak, corresponding to the melting point, except for extrudate A2.

In Fig. 18 (d), it is possible to visualize multiple peaks which could be contamination in the aluminium pan or an artifact caused by a change of heat transfer between sample and pan where the sample deforms or topples over in the pan or where the lid of the pan lifts off due to the release of vapours. This overlay of two peaks could also be explained by the existence of different crystal morphologies or several phase transitions. As described in Bialleck and Rein's work (33), the combination of starch and a lipophilic API, such as IBU, led to more complicated DSC thermograms with several phase transitions.
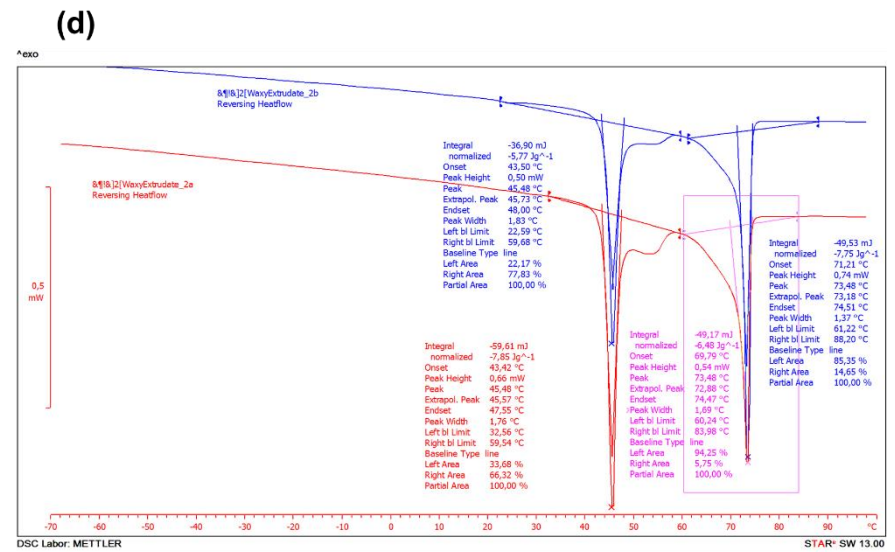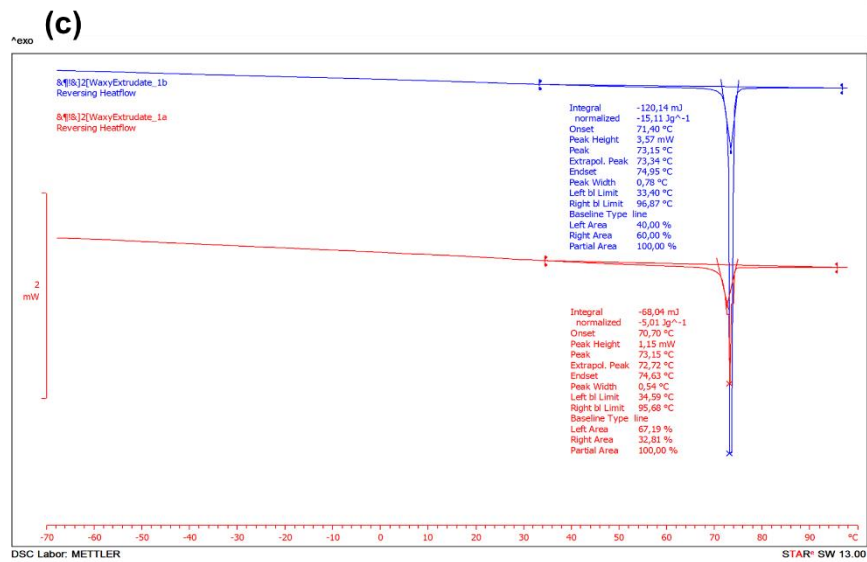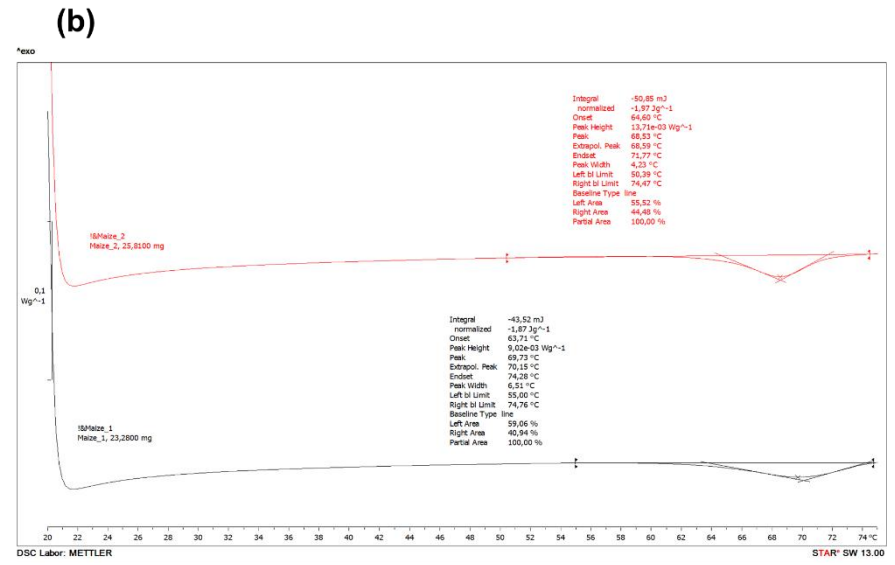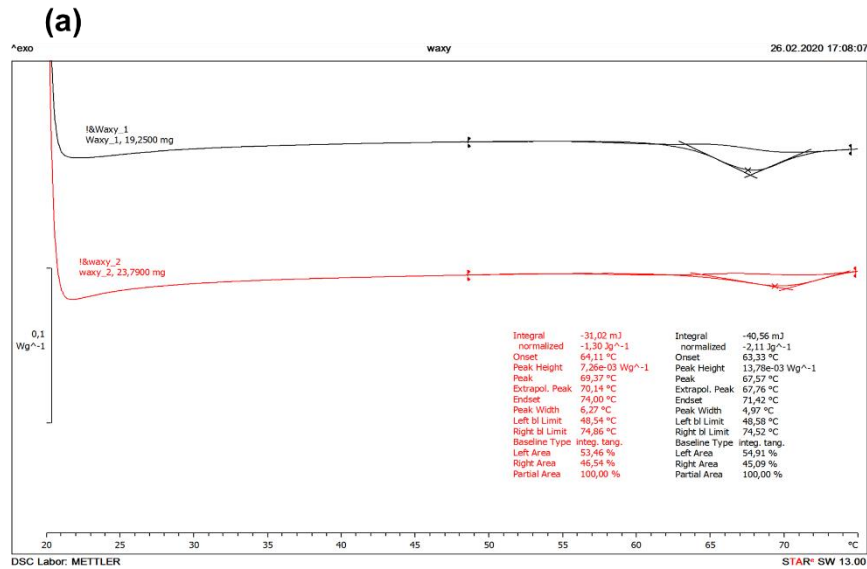
Figure 18. (a) Thermogram of neat Waxy Starch (b) Thermogram of neat maize Starch (c) Thermogram of extrudate A1 (d) Thermogram of extrudate A2.
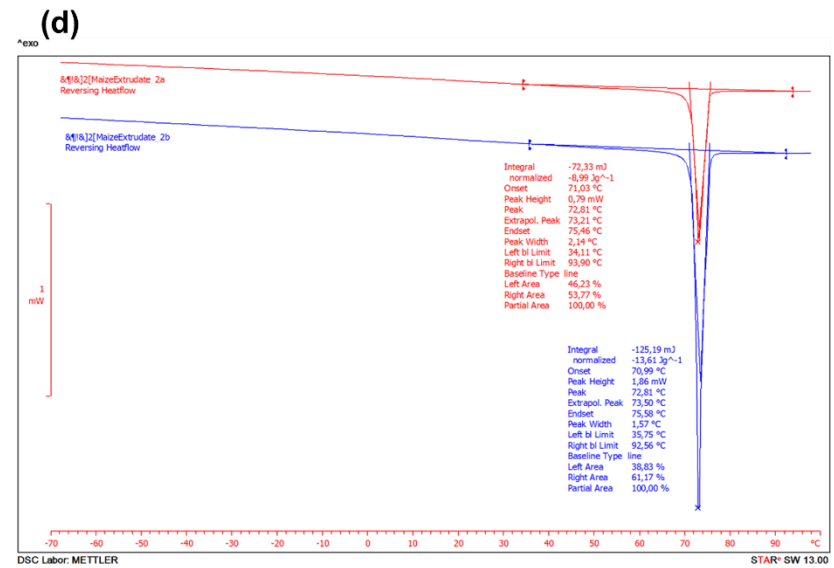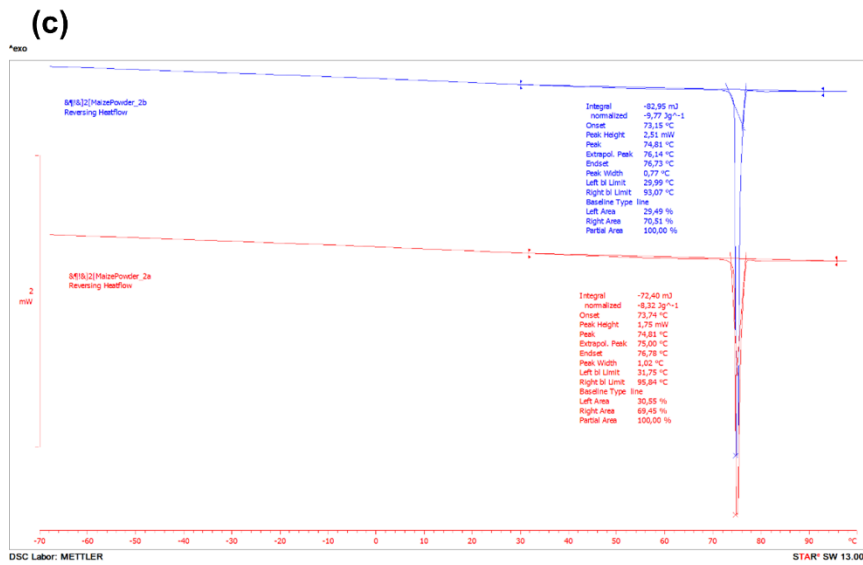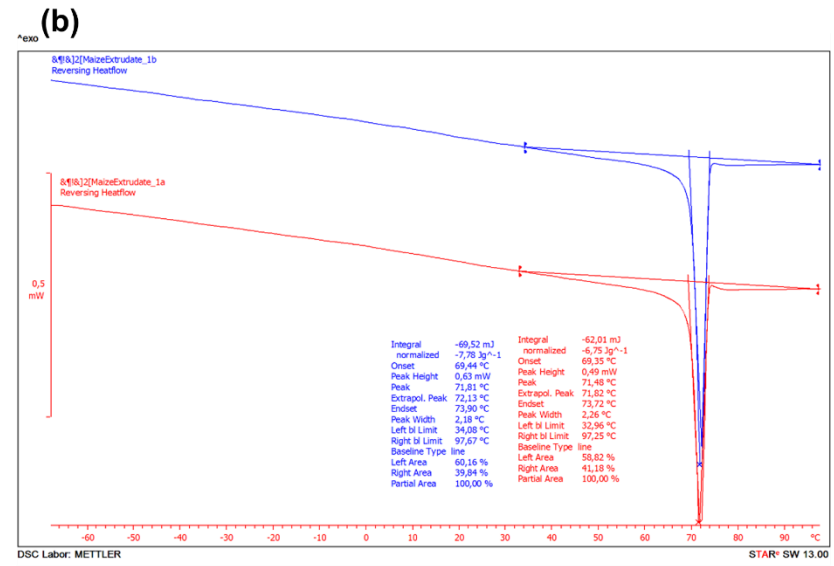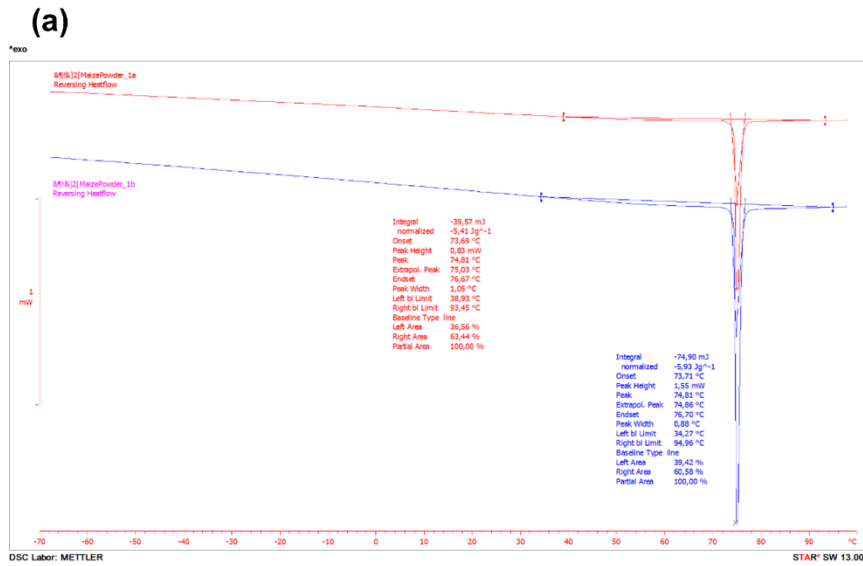
Figure 19. (a) Thermogram of AM1 physical mixture (b) Thermogram of extrudate AM1 (c) Thermogram of AM2 physical mixture (d) Thermogram of extrudate AM2.

50

4.4. Physicochemical properties of the Starches

Experimental T_g, onset (T_o), peak (T_p), and endset (T_e) for neat MS and WS values obtained by DSC are shown in Fig. 18 (a) and (b). This endotherm represents the transition of the polymer from the glassy to the rubbery state, which involves an enthalpy relaxation. Since the softening of a material requires heat, the heat capacity drops during the transition. The T_g of MS and WS are in agreement with the literature values. (33)

Copeland, Blazek, Salman, & Tang (31) reported that the gelatinization temperatures of most starches are observed to occur between 60 and 80 °C, which is consistent with the results. The theoretical T_g represents the real transition temperature value under an extremely slow heating rate, approaching zero. (30)

Liu et al. (22) show the gelatinization behavior of starch as a function of the collective melting properties of many individual crystallites of diverse stabilities and in different structural arrangements that make up granules, rather than being due to a concerted structural collapse taking place within the narrow DSC gelatinization endotherm. Regarding the mechanical stability and tensile strength of the extrudates, Kipping and Rein (18) reported that Waxy starch, an amylose-free starch, forms a more unstable matrix than Maize Corn Starch, although all of the extruded products exhibited a high mechanical resistance. They concluded that an increasing amount of amylose leads to a reinforcement of framework structure.

Moreover, the inter-relationship between water content, temperature and heating time played an important role in determining the degree of starch gelatinization. (22) Therefore, further investigation is required to understand the thermodynamic behaviour of starch.

4.5. Thermophysical characterization of IBU SD

The DSC curve of the PM exhibited a sharp endothermic peak at around 73 °C that was associated with the melting of IBU, which could be also detected in the IBU SD of different HME temperatures. The pure IBU melting point is 75 °C. The shift of the melting point is attributed to IBU's plasticizing effect.

The thermograms of IBU-WS SD and IBU-MS SD exhibited a single sharp endothermic peak, therefore it is reasonable to assume that the API remained in its crystalline form. The crystal melting endotherm in the thermograms above represents the heat flow into the sample. The area of the endotherm is the energy required for this transformation to generate a phase change.

4.6. Thermophysical characterization of CBZ SD

The thermograms of some runs of Table 2 and all of Table 3 extrudates, the SD with CBZ, are lacking due to insufficient time for further analyses and investigation caused by an early interruption of the research exchange period due to the COVID-19 pandemic.

5. Conclusion

The HME and ASD technologies have established themselves as promising approaches to increase the solubility of poorly water-soluble drugs and potentially to improve bioavailability.

ASD-based formulations can not only improve the oral bioavailability of poorly water-soluble drugs but also would enable more consistent pharmacokinetics by reducing variability; therefore, statistically significant clinical signals could be achieved using fewer subjects and shorter trials. Additionally, early implementation of ASD technology could help mitigate the risk of false termination of lifesaving drug candidates due to safety or efficacy issues that could simply be the result of erratic pharmacokinetics or poor bioavailability.

The Ibuprofen extruded filaments coming out of the die were not clear and translucent but opaque and white. The colour of the extrudate strands changes into a persistent white when the saturation limit is exceeded. Therefore, along with the information on the diffractograms and the thermograms, it is possible to say we produced a saturated IBU-starch dispersion in which Ibuprofen was dispersed in its crystalline form.

Moreover, attention should be paid to the amount of water used during the extrusion process, as insufficient quantities of water inhibit the starch gelatinization process and produced extrudate strands with "sharkskin", whereas a higher water content seems to favour amorphization, the HME process and the solid dispersions' formation.

Solid dispersions with carbamazepine can be produced at a lower temperature than the melting point of the API. Indeed, below the glass transition temperature starches are not completely gelatinized, whereas the risk of starch overcooking becomes unacceptable at very high temperatures and water contents, where bubbles appear on the exterior surface, as it was visible during the CBZ extrusion runs. The CBZ SD displayed a greyish colour and bubble-like areas at temperatures higher than 90 °C.

It is possible to claim the screws' speed has an impact in the amorphization of starch, revealing a more amorphous extrudate at a higher rpm value, according to the X-ray diffraction patterns of extruded neat Waxy Starch and the solid dispersions at different rpm. The present work confirmed that optimizing the HME process for complete amorphous conversion and minimal chemical deterioration is critical.

Concerning the relative crystallinity and the screw rotation speed parameter, at a speed of 200 rpm, the smallest amount of relative crystallinity was noticed, among the SD DCW and SD

DCM. Another important aspect is that comparing both starch types, SD with Maize Starch become less crystalline after HME.

The characteristic IBU and CBZ peaks have not disappeared in the solid dispersions' diffractograms. Typical peaks for crystalline IBU and CBZ, confirming that IBU and CBZ did not melt or solubilize in the polymer during the HME were observed by XRPD. It was hereby confirmed that it was not possible to produce a starch complete ASD with the model APIs.

The analysis of the thermograms indicates that there was not the creation of a glassy solution where the API is molecularly dispersed as proposed and intended.

In general, it can be concluded that the shift of the melting point in the IBU SD thermograms is attributed to IBU's plasticizing effect.

The combination of thermal and diffractometric methods allows a more detailed view of the thermomechanical properties of the polymeric system revealing important information about polymer–API interactions.

Overall, this work became a valuable learning experience in a foreign country and research institute. Although the results were not satisfactory, there was a lot to learn and take from this experience with the help of different professors and PhD students.

6. Future Perspectives

This study highlighted the potential of HME to overcome the poor aqueous solubility of many drugs with the use of a natural polysaccharide as the excipient. The impact of shear stress (screw speed and screw configuration), mean-residence time (e.g. throughput), viscosity of the melt, which also includes temperature, needs to be further investigated, as it likely has an additional impact on the SD attributes. More extrusion runs to find the optimal process conditions for these mixtures are in demand.

There are still many unknowns and it is key to obtain a deeper understanding with more experiments. The use of different grinding conditions, namely regarding the speed and typology of the grinding balls, should be evaluated consistently in the future.

Additional characterization methods could be helpful, for example, Fourier-transform infrared spectroscopy (FTIR) analysis, to investigate and describe interactions between starch, water and the APIs under investigation.

Maize corn starch revealed itself a better choice to produce amorphous solid dispersions, thus this starch type would be a preferential choice for further studies. Another starch type could also be considered.

The polymer–API solubility and miscibility essays and the biopharmaceutical assessment would have followed using bi-phasic dissolution testing of different size fractions of the milled extrudates with a focus on immediate release. Those experiments would also have been conducted if not for the COVID-19 pandemic, which unfortunately shortened the research time allocated to conduct this fieldwork.

Down-streaming of the formulations into final dosage forms, that is, capsules or tablets, is another important factor that needs to be considered in the future. The resulting solid dosage form is either a solid solution or a solid dispersion with low porosity, small surface area and large mechanical stability. Porosity measurements and relative density could be calculated with a pycnometer. Analysis via digital image could also be valuable to point out critical parameters influencing the quality. The stability evaluation by friability tests and by determining the tensile strength of the final products would also be important to perform.

The future will certainly bring further progress towards the rationalization of ASD technology, thereby creating superior products that lead to improved therapeutic outcomes.

7. References

1. Merna J, Mathers A, Hassouna F, Malinov L, Fulem M. Impact of Hot-Melt Extrusion Processing Conditions on Physicochemical Properties of Amorphous Solid Dispersions Containing Thermally Labile Acrylic Copolymer toslav R Kv e. 2020;109:1008–19.

2. Yu L. Amorphous pharmaceutical solids: preparation, characterization and stabilization. Adv Drug Deliv Rev. 2001;48:27–42.

3. Gala UH, Miller DA, Williams RO. Harnessing the therapeutic potential of anticancer drugs through amorphous solid dispersions. BBA - Rev Cancer [Internet]. 2020;1873(1). Available from: https://doi.org/10.1016/j.bbcan.2019.188319. Accessed on April 16th 2020.

4. Moseson DE, Taylor LS. The application of temperature-composition phase diagrams for hot melt extrusion processing of amorphous solid dispersions to prevent residual crystallinity. Int J Pharm. 2018;553(1–2):454–66.

5. Simo MF, Pereira A, Cardoso S, Cadonau S, Werner K. Five-Stage Approach for a Systematic Screening and Development of Etravirine Amorphous Solid Dispersions by Hot-Melt Extrusion. 2019;

6. Ziaee A, O'Dea S, Howard-Hildige A, Padrela L, Potter C, Iqbal J, et al. Amorphous solid dispersion of ibuprofen: A comparative study on the effect of solution based techniques. Int J Pharm. 2019;572(October).

7. Thiry J, Kok MGM, Collard L, Frère A, Krier F, Fillet M, et al. Bioavailability enhancement of itraconazole-based solid dispersions produced by hot melt extrusion in the framework of the Three Rs rule. Eur J Pharm Sci [Internet]. 2017;99:1–8. Available from: http://dx.doi.org/10.1016/j.ejps.2016.12.001. Accessed on April 24th 2020.

8. Karanth H, Shenoy VS, Murthy RR. Industrially Feasible Alternative Approaches in the Manufacture of Solid Dispersions : A Technical Report. 2006;7(4).

9. Solanki NG, Kathawala M, Serajuddin ATM. Effects of Surfactants on Itraconazole-Hydroxypropyl Methylcellulose Acetate Succinate Solid Dispersion Prepared by Hot Melt Extrusion III : Tableting of Extrudates and Drug Release From Tablets. J Pharm Sci [Internet]. 2019;108(12):3859–69. Available from: https://doi.org/10.1016/j.xphs.2019.09.014. Accessed on May 16th 2020.

10. Agrawal AM, Dudhedia MS, Zimny E. Hot Melt Extrusion: Development of an Amorphous Solid Dispersion for an Insoluble Drug from Mini-scale to Clinical Scale. AAPS PharmSciTech. 2016;17(1):133–47.

11. Raman V, Sarabu S, Bandari S, Batra A, Bi V, Durig T, et al. Stable amorphous solid dispersions of fenofibrate using hot melt extrusion technology: Effect of formulation and process parameters for a low glass transition temperature drug. J Drug Deliv Sci Technol [Internet]. 2020;58(August 2019):101395. Available from: https://doi.org/10.1016/j.jddst.2019.101395. Accessed on June

17th 2020.

12. Maniruzzaman, Mohammed, Boateng, Joshua S., Snowden, MartinJ., Douroumis D. A Review of Hot-Melt Extrusion: Process Technology to Pharmaceutical Products. 2012;(January 2018).

13. Censi R, Gigliobianco MR. Hot Melt Extrusion: Highlighting Physicochemical Factors to Be Investigated While Designing and Optimizing a Hot Melt Extrusion Process. Pharmaceutics. 2018;

14. Pitayachaval P, Watcharamaisakul P. A review of a machine design of chocolate extrusion based co-rotating twin screw extruder. Int Conf Informatics, Technol Eng. 2019;703:1–7.

15. Thiry J, Krier F, Evrard B. A review of pharmaceutical extrusion : Critical process parameters and. Int J Pharm. 2015;479(1):227–40.

16. Zhao Y, Xie X, Zhao Y, Gao Y, Cai C, Zhang Q, et al. Effect of plasticizers on manufacturing ritonavir / copovidone solid dispersions via hot-melt extrusion : Preformulation , physicochemical characterization , and pharmacokinetics in rats. Eur J Pharm Sci. 2019;127(June 2018):60–70.

17. Djuris J, Nikolakakis I, Ibric S, Djuric Z, Kachrimanis K. Preparation of carbamazepine – Soluplus solid dispersions by hot-melt extrusion , and prediction of drug – polymer miscibility by thermodynamic model fitting. 2013;84:228–37.

18. Kipping T, Rein H. A new method for the continuous production of single dosed controlled release matrix systems based on hot-melt extruded starch: Analysis of relevant process parameters and implementation of an in-process control. Eur J Pharm Biopharm. 2013;84(1):156–71.

19. Nakamichi K, Nakano T, Yasuura H, Izumi S. The role of the kneading paddle and the effects of screw revolution speed and water content on the preparation of solid dispersions using a twin-screw extruder. Int J Pharm. 2002;241:203–11.

20. Yeung C, Rein H. Determination of surface energies of hot-melt extruded sugar – starch pellets. Pharm Dev Technol. 2017;0(0):1–9.

21. Dedroog S, Pas T, Vergauwen B, Huygens C, Mooter G Van Den. Solid-state analysis of amorphous solid dispersions : Why DSC and XRPD may not be regarded as stand-alone techniques. J Pharm Biomed Anal. 2020;178:112937.

22. Liu Y, Yu J, Copeland L, Wang S, Wang S. Gelatinization behavior of starch: Reflecting beyond the endotherm measured by differential scanning calorimetry. Food Chem. 2019;284(29):53–9.

23. METTLER TOLEDO. TOPEM – Advanced Multi-Frequency Temperature Modulated DSC [Internet]. [cited 2020 Oct 24]. Available from: https://www.mt.com/in/en/home/library/videos/lab-analytical-instruments/topem-an-advanced-temperature-modulated-dsc-technique.html. Accessed on October 24th 2020.

24. Bunaciu AA, Udriştioiu E, Aboul-Enein HY. X-Ray Diffraction: Instrumentation and Applications. Crit Rev Anal Chem. 2015;8347:289–99.

25. Jayant S, Grohganz H, Rades T, Löbmann K. Recent advances in co-amorphous drug

formulations. Adv Drug Deliv Rev. 2016;100:116–25.

26.   Monnier X, Maigret J, Lourdin D, Saiter A. Glass transition of anhydrous starch by fast scanning calorimetry. Carbohydr Polym. 2017;

27.   Liu P, Yu L, Liu H, Chen L, Li L. Glass transition temperature of starch studied by a high-speed DSC. Carbohydr Polym. 2009;77(2):250–3.

28.   Chaudhary V, Payoyai N, M. Small D, Shanks RA, Kasapis S. Effect of the Glass Transition Temperature on alpha-amylase activity in a starch matrix. Carbohydr Polym. 2016;

29.   Kunle OO. Starch Source and Its Impact on Pharmaceutical Applications. Chem Prop Starch. 2019;1–14.

30.   Kipping T, Rita A, Pereira M, Rein H. The use of hot-melt extruded corn starch matrices as drug carrier systems : A thermophysical characterization. 2014;1–12.

31.   Copeland L, Blazek J, Salman H, Tang MC. Form and functionality of starch. Food Hydrocoll. 2008;23(6):1527–34.

32.   Willfahrt A, Steiner E, Hötzel J, Crispin X. Printable acid-modified corn starch as non-toxic, disposable hydrogel-polymer electrolyte in supercapacitors. Appl Phys A. 2019;125(7):1–10.

33.   Bialleck S, Rein H. Preparation of starch-based pellets by hot-melt extrusion. Eur J Pharm Biopharm. 2011;79(2):440–8.

34.   Yang Z, Hu Y, Tang G, Dong M, Liu Q, Lin X. Development of ibuprofen dry suspensions by hot melt extrusion: Characterization, physical stability and pharmacokinetic studies. J Drug Deliv Sci Technol. 2019;54(September):101313.

35.   Haque A, Hasan F, Dewan I, Islam SMA, Bhuiyan MA. Studies to Improve Dissolution Properties of Poorly Soluble Carbamazepine by Solid Dispersion. Bangladesh Pharm J. 2012;15(July):73–7.

36.   Royal Society of Chemistry. Carbamazepine [Internet]. ChemSpider database. 2020. Available from: http://www.chemspider.com/Chemical-Structure.2457.html. Accessed on May 25th 2020.

37.   Heena A, Shetty AA, Mehta CH, Nayak UY, Mutalik S, Pai KG. Solubility and Dissolution Improvement of Carbamazepine by Various Methods. Res J Pharm Tech. 2019;12(July):3618.

38.   Tolou-Ghamari Z, Zare M, Habibabadi JM NM. A quick review of carbamazepine pharmacokinetics in epilepsy from 1953 to 2012. J Res Med Sci. 2013;18(March):S81-5.

39.   Bochmann ES, Üstüner EE, Gryczke A, Wagner KG. Predicting melt rheology for hot-melt extrusion by means of a simple Tg -measurement. Eur J Pharm Biopharm. 2017;119:47–55.

40.   Bialleck S, Rein H. Drug release mechanisms of hot-melt extruded starch-based pellets. 2012;408–19.

41.   X-ray diffraction techniques in transmission geometry [Internet]. Malvernpanalytical.com. [cited 2020 Apr 22]. Available from: https://www.malvernpanalytical.com/en/learn/events-and-

training/webinars/W130712XrdTechniquesInTransmissionGeometry. Accessed on May 19th 2020.

42. Gryczke A, Schminke S, Maniruzzaman M, Beck J, Douroumis D. Development and evaluation of orally disintegrating tablets (ODTs) containing Ibuprofen granules prepared by hot melt extrusion. Colloids Surfaces B Biointerfaces. 2011;86(2):275–84.

43. Malwade C, Qu H, Rong B. Evaporative Crystallization of Carbamazepine from Different organic solvents. 20th Int Work Ind Cryst. 2013;(August 2015):364–71.

44. Steffens KE, Wagner KG. Dissolution enhancement of carbamazepine using twin-screw melt granulation. Eur J Pharm Biopharm. 2020;148(January):77–87.

45. Particle Technology Labs. Differential Scanning Calorimetry (DSC) [Internet]. Available from: https://www.particletechlabs.com/analytical-testing/thermal-analyses/differential-scanning-calorimetry. Accessed on October 26th 2020.

46. Royal Society of Chemistry. Ibuprofen [Internet]. ChemSpider database. 2020. Available from: http://www.chemspider.com/Chemical-Structure.3544.html. Accessed on October 27th 2020.

8. Appendix
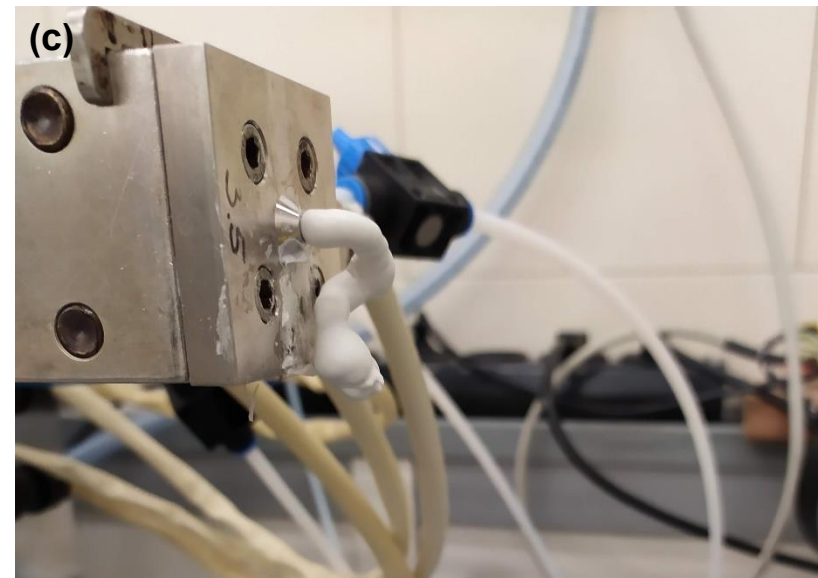
Appendix 1: Common defects observed in extrudates. (a) AM1 extrudate strand exiting the end-plate die. "Sharkskin effect" visible. (b) AM2 extrudate strand exiting the end-plate die. "Sharkskin effect" visible. (c) DCW 200 rpm extrudate strand exiting the end-plate die. Bubble-like areas visible.